https://doi.org/10.5194/egusphere-2026-1532
Preprint. Discussion started: 30 March 2026

Southern African dust aerosols are rich in micronutrients, K-feldspar and carbonate minerals

Clarissa Baldo[1], Servanne Chevaillier[1], Sophie Nowak[2], Gael Noyalet[1], Sandra Lafon[1], Claudia Di Biagio[1], Amelie Chaput[3,a], James King[3], Mathieu Cazaunau[4], Edouard Pangui[4], Jean-Francois Doussin[4], Remi Stanus[5,6], Nadine Mattielli[5], Heleen C. Vos[7], Gregory S. Okin[8], Brigitte Language[9], Stuart Piketh[9], Karine Desboeufs[1], Akinori Ito[10], Silvia Becagli[11], Laurie Barrier[12], Stephane Jacquemound[12], Paola Formenti[1]

[1] Université Paris Cité and Univ Paris Est Créteil, CNRS, LISA, F-75013 Paris, France
[2] Université Paris Cité, CNRS, ITODYS, Paris F-75013, France
[3] Department of Geography, Université de Montréal, Montréal, H2V0B3, Canada
[4] Univ Paris Est Créteil and Université Paris Cité , CNRS, LISA, F-94010 Créteil, France
[5] Laboratoire G-Time, Département Géosciences, Environnement et Société (DGES), Université Libre de Bruxelles (ULB), Av. F. Roosevelt, 50 (CP 160/02), Brussels, 1050, Belgium
[6] Archaeology, Environmental Changes & Geo-Chemistry Research Group, Vrije Universiteit Brussel, Pleinlaan 2, 1050 Brussels, Belgium
[7] Department of Earth Sciences, Stellenbosch University, Stellenbosch 7600, South Africa
[8] Department of Geography, University of California – Los Angeles, Los Angeles, California, USA
[9] Unit for Environmental Sciences and Management, North-West University, Potchefstroom 2520, South Africa
[10] Yokohama Institute for Earth Sciences, JAMSTEC, Yokohama, Kanagawa 236-0001, Japan
[11] Department of Chemistry "Ugo Schiff", University of Florence, Italy
[12] Institut de physique du globe de Paris, Université Paris Cité, UMR CNRS 7154, 1 rue Jussieu, 75005 Paris, France
[a] Now at Department of Civil and Environmental Engineering, National University of Singapore, 117576, Singapore.

Correspondence to: Clarissa Baldo (clarissa.baldo@lisa.ipsl.fr)

Abstract. This study provides the first comprehensive characterisation of the chemical and mineralogical composition of mineral dust from Southern Africa, a major global dust source with significant impacts on regional climate and marine ecosystems. Laboratory-generated dust aerosol samples were produced using soils collected from key natural and emerging anthropogenic dust sources in Southern Africa.

The chemical properties of mineral dust across Southern Africa were characterised using the elemental ratios Si/Al, (Ca + Mg)/Al, and K/Al, together with clay content. These indicators distinguish dust aerosols originating from arid western coastal areas from those originating from more humid eastern inland regions. They also provide information about the source-area environments and sediment weathering regimes, which are influenced by current and past temperature and precipitation patterns.

The results of this study indicate that Southern African dust contains essential micronutrients such as iron (Fe), phosphorus (P) and manganese (Mn), which can become soluble and bioaccessible during atmospheric transport. This affects the biogeochemistry of nearby and remote marine ecosystems, including the Southern Ocean. Southern African dust also contains higher levels of carbonates than Northern African dust sources, which can promote heterogeneous reactions and

https://doi.org/10.5194/egusphere-2026-1532
Preprint. Discussion started: 30 March 2026

particle ageing, and contribute to cloud condensation nuclei in the extensive stratocumulus deck over the northern Bay of Benguela. Our findings also suggest that Southern African dust contains higher levels of K-feldspar than Northern African dust, and could therefore be an important source of ice-nucleating particles for low mixed-phase clouds over the Southern Ocean.

1 Introduction

Southern Africa has a significant influence on the mineral dust budget of the Southern Hemisphere. The southernmost region of the African continent, comprising Botswana, Lesotho, Namibia, and South Africa, encompasses a range of arid and semi-arid landscapes, including vast deserts, ephemeral riverbeds and lakes, and shrublands (Eckardt et al., 2020; Ginoux et al., 2012; Vickery et al., 2013; Vos et al., 2025). These environments are susceptible to wind erosion, which lifts mineral dust particles from exposed soils into the atmosphere. Model estimates suggest that Southern Africa accounts for around 20% of global emissions, though there is significant uncertainty surrounding this figure (Kok et al., 2021).

Currently, Southern Africa is experiencing progressive temperature rises and worsening drought conditions. The severe 2023/24 droughts that prompted national emergencies are evidence of this (United Nations South Africa 2024). Regional temperatures are projected to rise by 4-5 °C above pre-industrial levels by the end of the century (Engelbrecht et al., 2015; Trisos et al., 2022), and mineral dust emissions are also expected to increase (Liu et al., 2024).

Drought, vegetation loss, and the decline of surface bio-crusts are accelerating land degradation due to climate change and land-use changes (Rodríguez-Caballero et al., 2022). Moreover, despite its low average population density, Southern Africa is under strong anthropogenic pressure due to rapid urbanisation and industrialisation (Gambe et al., 2023; Matthaios et al., 2025). This creates new dust hotspots, including in agricultural areas in the Free State in central South Africa (Eckardt et al., 2020; Trisos et al., 2022; Vickery et al., 2013) and in the semi-arid shrublands along the west coast of South Africa (Vos et al., 2025). Extensive savannah areas in Southern Africa are highly vulnerable to climate and anthropogenic pressures and can produce prolonged post-fire dust outbreaks in areas that are normally dust-free (Yu and Ginoux, 2022). Intensive mining activities across Southern Africa (Cole, 2024; Mhlongo, 2023) can also contribute to the release of mineral dust from active and abandoned sites.

The period of highest dust event frequency generally occurs during the cold and dry seasons, with some exceptions, such as the west coast of South Africa, where winter is also a rainy season. Between April and September, widespread dust sources along the Namibian coast, including the Central Namib Gravel Plain and ephemeral riverbeds, are activated by the Berg winds blowing in from the east (Vickery et al., 2013). A similar temporal pattern is observed for dust sources on the west coast of South Africa, with dust events also occurring in November and February (Vos et al., 2025). Inland sources, including the Makgadikgadi Pans in northeastern Botswana, the Etosha Pan in northeastern Namibia, and smaller pans in the southwestern Kalahari across Namibia and South Africa, are active between May and November, peaking around August

https://doi.org/10.5194/egusphere-2026-1532
Preprint. Discussion started: 30 March 2026

(Vickery and Eckardt, 2013). Dust events in the Free State occur from June to January, peaking in August, September and November (Eckardt et al., 2020).

The presence of diverse landscape types, together with the strong influence of climate change and human activity on these environments, makes it difficult to estimate mineral dust emissions from Southern Africa with any certainty, especially given the limited observational data on dust aerosols and the resulting lack of constraints (Leung et al., 2025). Consequently, Southern Africa remains a significant knowledge gap in the mineral dust budget of the Southern Hemisphere.

The potential impacts of Southern African (SAf) dust could extend beyond its source areas. Mineral dust plays a key role in biogeochemical processes, as the nutrients it contains can fertilise marine ecosystems and affect carbon storage (Jickells et al., 2014). SAf dust can be transported over long distances across the subcontinent towards the nearby South Atlantic and Indian Oceans and the remote Southern Oceans (Ito and Miyakawa, 2023; Liu et al., 2022; Matsui et al., 2018; Piketh and Walton, 2004), reaching even Antarctica (Gili et al., 2022).

During long-range transport, nutrients in dust can become soluble through interactions with gaseous pollutants and mixing with atmospheric aerosols from marine, anthropogenic, and biomass-burning sources, which makes them bioaccessible to marine ecosystems. Aerosols mixed with dust over the Namibian coast exhibit around 20%-Fe solubility, which is significantly higher than the typical <1% in dust from near global dust source areas due to marine biogenic processing (Desboeufs et al., 2024). Recent research suggests that SAf dust is important for phytoplankton productivity in the adjacent Benguela Upwelling System off the Namibian coast, which is one of the most productive regions of the global oceans (Belelie et al., 2025). In addition, the transport of SAf dust has been linked to exceptionally strong phytoplankton blooms (Gittings et al., 2024) and may be a key source of Fe in remote, nutrient-limited areas of the Indian and Southern Oceans (Gili et al., 2022; Gittings et al., 2024).

SAf dust can also contribute to the hemispheric radiative budget by supplying particles that scatter, absorb, and transmit solar and terrestrial radiation (Kok et al., 2017). Additionally, they can modify cloud properties and lifetimes, as mineral dust facilitates the formation of cloud droplets and ice crystals within clouds (Karydis et al., 2017; Storelvmo, 2017). Tesfaye et al. (2015) estimated that mineral dust over the subcontinent could exert a strong shortwave radiative effect. This would decrease surface solar radiation by 8.2 W m^{-2} (regional annual mean) and warm the atmosphere by 4.5 W m^{-2}, leading to increased cloud cover and changes in the structure of the planetary boundary layer.

SAf dust can supply cloud condensation nuclei (CCN) to the low-level stratocumulus cloud deck in the northern Benguela Upwelling System. These clouds produce strong negative radiative forcing by reflecting solar radiation. This affects the energy balance and surface temperature of the South Atlantic Ocean, as well as large-scale atmospheric circulation and precipitation (Formenti et al., 2019 and references therein).

SAf dust is an important source of ice-nucleating particles (INPs) in low-level mixed-phase clouds over the Southern Ocean and may influence the regional radiative budget. INP concentrations in this region are very low due to the absence of local Antarctic sources (Wex et al., 2025), with around 30% of the dust mass and INP numbers attributable to SAf dust (Kawai and Matsui, 2025). These findings are consistent with those of Chen et al. (2025), who reported that mineral dust exhibits

https://doi.org/10.5194/egusphere-2026-1532
Preprint. Discussion started: 30 March 2026

significantly higher INP activity than carbonaceous aerosols from biomass and fossil fuel combustion. Consequently, although both aerosol types are transported to the Southern Ocean, mineral dust is likely the dominant source of INP.

Modelling estimates suggest that SAf dust could also account for up to 8% of total dust deposition in Antarctica (Kok et al., 2021). This would affect the regional climate of this sensitive region, which is warming 3 times faster than the global average (Clem et al., 2020), for example, by reducing surface albedo and accelerating the melting of snow and ice (Skiles et al., 2018).

It is essential to assess the chemical composition and mineralogy of mineral dust particles to model dust aerosol properties and evaluate their impacts. This includes their role in (1) supplying key nutrients such as iron (Fe), phosphorus (P), and manganese (Mn) (Hamilton et al., 2022; Lu et al., 2024), (2) participating in heterogeneous chemical reactions, for example, in the presence of TiO_2 and carbonate particles, which promote particle ageing through coating after gaseous pollutants uptake (Chen et al., 2012; Krueger et al., 2004), (3) contributing light-absorbing minerals such as Fe oxide, which have main absorption bands in the solar spectrum (Caponi et al., 2017; Derimian et al., 2008; Di Biagio et al., 2019; Lafon et al., 2006), but also carbonates, gypsum, quartz, and clays, which have main absorption bands in the thermal infrared (Di Biagio et al., 2017; Engelbrecht et al., 2016; Sokolik and Toon, 1999), and (4) providing ice-nucleating particles such as K-feldspars (Harrison et al., 2016; Zolles et al., 2019). Compositional information, such as crustal element ratios and clay mineral contents, is often used for source attribution (Formenti et al., 2014; Scheuvens and Kandler, 2014; Scheuvens et al., 2013). This improves our understanding of the transport and deposition patterns of different source types and consequently their relative impacts on the radiation balance.

However, observations of the chemical properties of SAf dust are limited. Laboratory and field studies have reported on the chemical composition of aerosols in various locations, including the Central Namib Gravel Plain (Di Biagio et al., 2017; Eltayeb et al., 1993; Qu, 2016), the western Kalahari in central Namibia (Qu, 2016), the Etosha and Makgadikgadi Pans (Engelbrecht et al., 2016), and the Okavango Delta in northeastern Botswana (Humphries et al., 2014). However, the available data often relate to a limited number of samples and elemental ratios. Observations of the mineralogy of SAf dust are restricted to a few samples from the Central Namib Gravel Plain (Di Biagio et al., 2017). A few studies have investigated mineral dust from ephemeral rivers, but they either focus on soil fractions that might not be representative of the emitted dust composition due to mineral fractionation during emission or provide dust elemental composition limited to Fe and P (Dansie et al., 2018; Dansie et al., 2017a; Dansie et al., 2017b). To the best of our knowledge, there are no observations of the chemical composition or mineralogy of anthropogenic mineral dust sources in Southern Africa.

This paper presents new observations on the chemical and mineralogical composition of mineral dust aerosols in Southern Africa, and it includes the first assessments of a small number of emerging anthropogenic dust sources. This study is based on the analysis of laboratory-generated dust aerosols from parent soils collected in key dust source areas. We analysed crustal elements and minerals and conducted a comprehensive review of observations from across Southern Africa. These were then compared with some of the major global dust sources. Our results provide new insights into the chemical

https://doi.org/10.5194/egusphere-2026-1532
Preprint. Discussion started: 30 March 2026

properties of Southern African dust aerosols and evaluate their potential implications for regional climate and marine ecosystems.

2 Methodology

Soil samples from major and emerging dust source areas in Southern Africa were used in laboratory experiments to generate dust aerosols. The aerosol samples were then analysed to determine their chemical and mineralogical compositions. Here, we describe the primary dust source areas in Southern Africa and the soil collection sites for this study (Fig. 1). The experimental setup for generating dust aerosols and their chemical characterisation is outlined. Additionally, we review the literature on Southern African dust sources and other major source regions, compiling an integrated dataset of mineral dust composition and mineralogy. Details of the laboratory-generated aerosol samples from this study are provided in Table S1, including the locations and geographic coordinates of the corresponding soils, the system used for the aerosol generation, and the availability of chemical and mineralogical data.

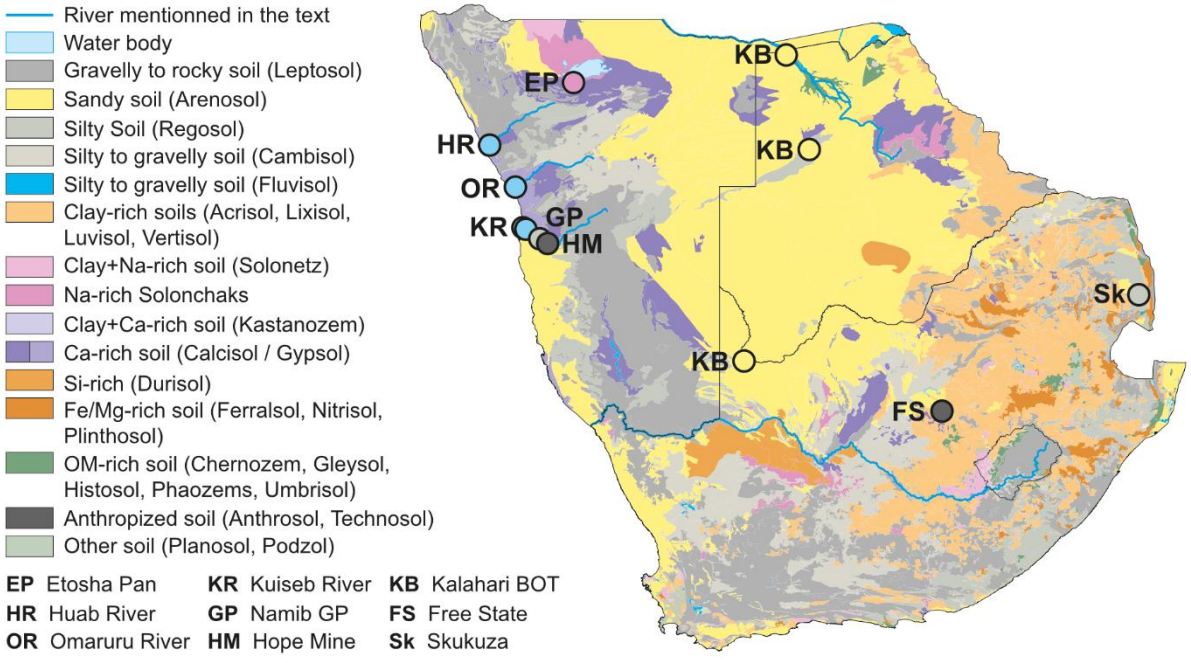

Figure 1. Sample location and pedological setting. The soil map is modified from Jones et al. (2013). OM is for Organic matter, GP for Gravel Plain and BOT for Botswana.

https://doi.org/10.5194/egusphere-2026-1532
Preprint. Discussion started: 30 March 2026

2.1 Soil sampling sites and description of the study area

Surface sediment samples were collected from the main and emerging dust source areas in Southern Africa by sampling only the top few centimetres of the surface, as this layer contributes to aerosol production. Soil collection sites include the Etosha Pan, the Central Namib Gravel Plain and the Kuiseb riverbed at the Gobabeb Namib Research Centre, the southwestern Kalahari in southwestern Botswana, areas of the Kalahari Desert north and south of the Okavango Delta in northwestern Botswana, agricultural soils in the Free State, savannah soils at Skukuza in the Kruger National Park in South Africa, and samples from an abandoned copper mine, Hope Mine in Namibia (Fig. 1 and Table S1). Furthermore, soil samples from the terminal reaches of the Huab, Kuiseb, and Omaruru rivers were collected along 1-km riverbed transects at 100-m intervals to ensure representativeness (Fig. 1 and Table S1).

Previous studies have documented the primary sources of mineral dust in Southern Africa (Eckardt et al., 2020; Ginoux et al., 2012; Vickery et al., 2013; Vos et al., 2025), which are summarised herein. The Namib Desert extends more than 2,000 kilometres from Angola to South Africa, over a ~150-km-wide area along the Atlantic Ocean coast (Fig 1). Inland, this coastal desert slopes ~0.5° from sea level to the west to approximately 1,000 metres a.s.l. to the east, where it is bounded by the Great Escarpment. This escarpment is a major topographic step of several 100s-m-high that separates the coastal areas surrounding Southern Africa from a high plateau, the South African Plateau, in the centre of the continent, with an average elevation of ~1700 m. On the Atlantic side, the aridity of the Namib Desert is due to a combination of the southern subtropical high-pressure belt, where cold and dry air masses of the Hadley and Ferrel atmospheric convection cells subside to the ground, and the cold Benguela current, which causes upwelling of cold water along the coast and limits sea surface evaporation (Diester-Haass et al., 1988; Mendelsohn et al., 2022; Stuut et al., 2004). Consequently, the desert experiences irregular precipitation, receiving less than 100 mm of rain per year, with the 100-mm isohyet running parallel to the Great Escarpment. Near the coast, frequent fogs supply moisture, supporting terrestrial ecosystems (Desmet, 2007; Desmet and Cowling, 1999; Olivier, 1995). Local geomorphology is shaped by aeolian, fluvial, and marine erosion, sediment transport, and sedimentation, with mechanical weathering prevailing over chemical weathering (Scholz, 1972; Watson and Lemon, 1985).

On the Great Escarpment, a series of watersheds feed ephemeral rivers that flow westward across the desert toward the ocean. The Kuiseb River divides the southern Namib Sand Sea from the Central Namib Desert Gravel Plain (hereafter referred to as Namib GP, Fig.1). Silty deposits are widespread in this gravel plain, which extends from the Skeleton Coast erg, a dune belt running along the coastline, up the edge of the Great Escarpment. These loess deposits are supplied by ephemeral rivers and by wind-blown dust from the western Kalahari, located on the South African Plateau to the east of the Namib Desert (Eitel et al., 2001; Scholz, 1972; Watson and Lemon, 1985). They cover the Protero-Paleozoic crystalline basement, which is composed of igneous and metamorphic rocks of the Damara Supergroup, forming inselberg-like topography characterised by isolated rocky outcrops (Watson and Lemon, 1985). These loess deposits are a significant source of mineral dust, with numerous point sources on the Namib GP, including riverbeds and coastal pans (Ginoux et al.,

https://doi.org/10.5194/egusphere-2026-1532
Preprint. Discussion started: 30 March 2026

2012; Vickery et al., 2013). In particular, the Huab, Kuiseb, and Omaruru rivers were recognised as the three dustiest river systems within the Namib Desert (von Holdt et al., 2017).

In the centre of the continent, the South African Plateau receives over 300 mm of rainfall per year and supplies tributaries of the Orange River flowing southwards, as well as ephemeral rivers that drain eastwards and northwards into large endorheic depressions of the Kalahari Basin (Watson and Lemon, 1985). In these depressions, the Makgadikgadi Pan in northeastern Botswana and Etosha Pan in northeastern Namibia are two of the largest paleolakes in Africa. Their highly dynamic surfaces are characterised by a crust of evaporite minerals and clays, which serve as major sources of dust globally (Buch and Rose, 1996; Vickery and Eckardt, 2021), although emissions are intermittent due to precipitation and complex salt-basin dynamics (Bryant, 2003; Bryant et al., 2007; Haustein et al., 2015). In addition, upstream of the Makgadikgadi Pan, the fluvial Okavango Delta in northwestern Botswana is also considered an important local dust source (Bullard, 2004; Vickery et al., 2013).

The Kalahari Basin is covered by the sediments of the Kalahari Desert that, at the surface, primarily consist of quartz-rich sands, forming an extensive, continuous sand sea, the largest on Earth. The northern and central parts of the Kalahari contain pure quartzose sand and clay minerals, indicating a strong weathering regime under a humid past climate (Garzanti et al., 2022). However, sediment compositions vary notably at the western and eastern edges of the desert, where rivers flow across different crystalline basement lithologies in Southern Africa. In the western Kalahari, dune fields in southeastern Namibia are distinguished by their enrichment in feldspar, which is thought to be the result of the influence of the Damara Supergroup rocks (Garzanti et al., 2022). The Kalahari Desert is also characterised by duricrusts – chemical precipitates of carbonates or silica, which are commonly found in pans and river valleys (Garzanti et al., 2022; Nash and McLaren, 2003). In addition to the large endorheic watersheds in the north, the southern Kalahari is an important dust source area due to numerous active pans in the southwestern Kalahari across Namibia and South Africa (Vickery and Eckardt, 2013). Furthermore, interdunes in the southern Kalahari, enriched with fine sediments, are emerging as a dust source as savannah-covered dune fields are being remobilised by overgrazing and drought (Bhattachan et al., 2012; Bhattachan et al., 2013).

Several areas in South Africa have also been identified as sources of dust. Mineral dust emissions are increasingly affected by human activities, especially in the Free State (Eckardt et al., 2020; Trisos et al., 2022; Vickery et al., 2013), characterised by intensive agriculture, and along the west coast, with vulnerable semi-arid shrubland environments and extensive mining (Vos et al., 2025). Furthermore, frequent fires in the grasslands and savannahs of northeastern and eastern South Africa (Strydom and Savage, 2016) contribute to vegetation loss, land degradation, and the emergence of new mineral dust sources.

2.2 Experimental setup

2.2.1 Dust aerosol generation

The “Générateur d’Aérosol Minéral En Laboratoire” (GAMEL, Lafon et al., 2014) was used to generate dust aerosols from parent soil samples. A mechanical wrist-action shaker (Agitest®, 8 mm amplitude) simulated the wind-driven movement of

https://doi.org/10.5194/egusphere-2026-1532
Preprint. Discussion started: 30 March 2026

soil grains, thereby reproducing the effect of sandblasting. Around 1-3 g of 1000 µm-sieved soil was agitated in a Büchner flask for 3-12 min at shaking frequencies of 500-650 cycles/min, depending on the observed dust generation efficiency of the soils. The airborne dust aerosols released from the parent soils were drawn through tubing into a size-selective cyclone device (URG-2000-30EA, URG Corporation, Chapel Hill, NC, USA) at a controlled flow rate for PM_{10} sampling (particles with an aerodynamic diameter of less than 10 µm).

For the soil samples collected at the terminal parts of the Huab, Kuiseb, and Omaruru riverbeds, dust aerosols were generated using the Multiphase Atmospheric Experimental Simulation Chamber (CESAM, Wang et al., 2011). This facility has been widely used to characterise the chemical and physical properties of natural mineral dust aerosols (Baldo et al., 2023; Baldo et al., 2020; Caponi et al., 2017; Di Biagio et al., 2014; Di Biagio et al., 2019; Di Biagio et al., 2017). The dust aerosol generator coupled to CESAM comprised a sieve shaker (Retsch AS200) that agitated a Büchner flask containing about 10 g of soil (sieved to 1000 µm and dried at 100°C for about 1 hour). The dust particles released by mechanical shaking were injected into the simulation chamber via a nitrogen carrier gas (10 L min^{-1}) for about 20 minutes. The particles remained suspended for approximately 3 hours, during which time they were characterised using several online and offline instruments.

Measuring the size distribution at both facilities allows comparison between the datasets. The GAMEL system hosts a GRIMM optical particle counter (OPC, Grimm Inc. model G1.108, light source operating at 780 nm, optical-equivalent diameter range 0.3-20 µm, 1.2 L min^{-1} flow rate, 6-sec time resolution), connected to the manifold used for filter sample collection.

The size distribution of dust particles suspended in CESAM was monitored using a combination of three instruments, including a scanning mobility particle sizer (SMPS, TSI, DMA model 3080 and CPC model 3772; mobility diameter range: 0.019-0.882 µm; sheath/aerosol flow rate: 2.0/0.2 L min-1; time resolution: 135 s), a SkyGRIMM OPC (Grimm Inc. model 1.129, light source: 655 nm, optical-equivalent diameter range: 0.25-32 µm, flow rate: 1.2 L min^{-1}; time resolution: 6 s) and a WELAS OPC (PALAS, model 2000; white light source: 0.35 to 0.70 µm; optical-equivalent diameter range: 0.58–40.7 µm; flow rate: 2 L min^{-1}; time resolution: 60 s).

The generated dust aerosols follow a single-mode log-normal distribution peaking between 3.2 and 9.8 µm. This is consistent with the atmospheric measurements reported by Formenti and Di Biagio (2024) near source regions (Fig. S1). The only exception is the aerosol sample generated in CESAM from Kuiseb River sediments, which exhibits an additional peak at 1 µm, which is absent in dust aerosols generated using GAMEL. The reason for this difference is unknown, but it is within the bounds of experimental uncertainty. The processing of the size distribution data is detailed in Text S1.

2.2.2 Filter sample collection

To investigate the chemical and mineralogical composition of the PM_{10} aerosol, samples were collected on 37 mm diameter, 0.4 µm-pore-size polycarbonate filters, using custom-made filter holders operated in parallel (Caponi et al., 2017).

https://doi.org/10.5194/egusphere-2026-1532
Preprint. Discussion started: 30 March 2026

During the GAMEL experiments, three filter samples were collected at a flow rate of 10 L min^{-1} each. For each soil sample, experiments were repeated until an optimal dust mass had accumulated on the filters for chemical analysis by X-ray fluorescence (XRF, around 500 ug) and for mineralogical analysis by X-ray diffraction (XRD, around 800 ug).

Two filter samples were collected during the CESAM experiments. Filters for mineralogical analysis were sampled at a flow rate of 9 L min^{-1} for about 1 hour, while those for chemical analysis were sampled at a flow rate of 3 L min^{-1} over the same period. The target dust mass for XRD analysis was achieved only for the Huab soil. For the Kuiseb and Omaruru experiments, only chemical composition data are available. Table S1 lists the aerosol filter samples.

2.2.3 Composition Analyses

The XRF analyses were performed on the PRAMMICS platform at LISA. Dust aerosol samples from CESAM were analysed using a 2404 XRF spectrometer by Malvern Panalytical, while samples from GAMEL were analysed with a Zetium spectrometer also by Malvern Panalytical.

Excitation X-rays are produced by a Coolidge tube (Imax = 125 mA, Vmax = 60 kV) with a Rh anode; the primary X-ray spectrum can be controlled by inserting filters (Al, at different thicknesses) between the anode and the sample. Each element was analysed under specific conditions (i.e. voltage, tube filter, collimator, analysing crystal, and detector), with a duration of 8 to 12 s for sequential WD-XRF analyses and 120 s for simultaneous ED-XRF analyses.

Data were collected using the SuperQ software for up to 28 elements (by WD-XRF: Na, Mg, Al, Si, P, S, Cl, K, Ca, Ti, V, Cr, Mn, Te, Ba, Nd; by ED-XRF: Fe, Co, Ni, Cu, Zn, As, Se, Sr, Cd, Pb). The elemental mass thickness, that is the analysed elemental mass per unit surface (µg cm^{-2}), was obtained by comparing the filter yields with a sensitivity curve measured in the same geometry on a set of certified XRF calibration standards (Micromatter ™), then correcting the signal for light elements (Na to Ca) to account for self-attenuation of the X-ray signal within the particle (Baldo et al., 2020; Caponi et al., 2017; Formenti et al., 2010). These standards are prepared by vacuum deposition, resulting in a highly uniform deposit on a polycarbonate membrane. In most cases, the standards are free of interference and thin enough to ignore thickness effects. The materials used are 99.9% pure or better, and each standard thickness is certified to +/- 5%.

The total aerosol mass on the filters was calculated as the sum of the masses of the oxides of the major crustal elements (SiO_2, Al_2O_3, Fe_2O_3, CaO, MgO, K_2O, Na_2O, TiO_2, P_2O_5, MnO) as follows (Lide, 1992):

$$\text{Aerosol mass} = 2.14 \cdot [\text{Si}] + 1.89 \cdot [\text{Al}] + 1.43\,[\text{Fe}] + 1.40 \cdot [\text{Ca}] + 1.66 \cdot [\text{Mg}] + 1.21 \cdot [\text{K}] + 1.35 \cdot [\text{Na}] + 1.67\,[\text{Ti}] + 2.29\,[\text{P}] + 1.29\,[\text{Mn}] \quad (1)$$

This was used to estimate the weight percentages (wt%) of the element fractions in the dust. The uncertainty in the measured elemental concentrations is around 10% (Caponi et al., 2017), with quantification limits of 1-4 µg for Ca, Fe, K, and Nd, and 0-0.5 µg for the other elements. Data below detection limits were treated as zero in the statistical analysis of the specific region.

https://doi.org/10.5194/egusphere-2026-1532
Preprint. Discussion started: 30 March 2026

Furthermore, enrichment factors (EFs) were used to analyse differences in element enrichment relative to the Earth's crust. These were calculated by normalising the ratio of each element to Aluminium (Al) in mineral dust against the corresponding crustal ratio derived from Rudnick and Gao (2014). EF = 1 indicates that the element proportion is consistent with the average crustal proportion; EF > 1 indicates enrichment, while EF < 1 indicates depletion.

The XRD measurements were performed at the X-Ray ITODYS-LISA platform of Université Paris Cité, using a Panalytical Empyrean powder diffractometer equipped with a PIXcel detector and a Cu anode tube (Kalpha = 1.541874 Å) operating at 45 kV and 40 mA. The analysis approach follows Nowak et al. (2018) and comprises two steps to collect and process diffractograms for phase identification and quantification. This is the same approach used by Baldo et al. (2020) for mineralogical analysis of Icelandic dust aerosols. For the identification of mineral phases, diffractograms were recorded in the 4°–80° 2θ range over 2 hours. The samples were deposited onto a flat monocrystalline silicon wafer and then loaded into the reflection spinner sample holder with a 1-s rotation time. Mineral identification was performed using HighScore Plus 3.0 (Degen et al., 2014) and the ICSD-Pan (Inorganic Crystal Structure Database) and COD (Crystallography Open Database) databases.

For the quantitative analysis, diffractograms were recorded in the 3°-70° 2θ range over 15 hours. Each sample was introduced into a 1 mm-diameter borosilicate capillary to allow observation of all crystallographic orientations via rotational movement and to obtain the correct relative intensities in the diffractogram. The quantitative analysis was conducted using MAUD (Material Analysis Using Diffraction), an XRD program based on the Rietveld refinement method, which uses least-squares procedures to minimise differences between observed and calculated diffractograms (Lutterotti et al., 1999). The diffractograms of the mineral phases identified with HighScore Plus were loaded as references in MAUD. The Rietveld model refines n-1 phases. As the total is fixed at 100, the last phase is obtained by subtraction of the sum of the n refined phases. The analytical uncertainty for the refined phases is estimated by the software and represents the lower limit of the uncertainty in the proportion of each identified mineral. The quality of the fit is evaluated using the reduced chi-square (χ^2) calculated by the model, which should be close to one for a good fit (although small χ^2 values can occur when a large percentage of the intensity comes from the baseline), and by visually comparing the observed and calculated diffractograms to achieve a realistic chemical model (Toby, 2006). The overall uncertainty in the measured mineral concentrations is around 10%. The estimated mineral contents are reported as wt%.

2.3 Integrated Dataset Compilation

We compiled an integrated dataset from this study and the existing literature on the chemical and mineralogical composition of mineral dust aerosols in Southern Africa, Australia, and Southern America. These three source regions are important for the mineral dust budget of the Southern Hemisphere. Additionally, we included Northern Africa, the main contributor to global mineral dust emissions (Kok et al., 2021). Table S2 provides key references for each dust source region, including details of the study area, aerosol collection method, particle size, available data (i.e. elemental and/or mineralogical composition), and the analytical technique used in each study.

https://doi.org/10.5194/egusphere-2026-1532
Preprint. Discussion started: 30 March 2026

To the best of our knowledge, literature on the mineralogical composition of SAf dust and more broadly on mineral dust in the Southern Hemisphere is limited. Consequently, we could only integrate our data with laboratory observations from Di Biagio et al. (2017). However, numerous studies report on the mineralogical composition of dust from Northern Africa (e.g. Di Biagio et al., 2017; Engelbrecht et al., 2016; Formenti et al., 2014; Formenti et al., 2008; Klaver et al., 2011).

Available data on the chemical composition of SAf dust include studies on the Namib GP (Di Biagio et al., 2017; Eltayeb et al., 1993; Qu, 2016), the western Kalahari in central Namibia (hereafter referred to as Kalahari NAM, Qu, 2016), the Etosha and Makgadikgadi Pans (Engelbrecht et al., 2016), and the Okavango Delta (Humphries et al., 2014). In Southern America, most dust observations come from Patagonia (Demasy et al., 2024; Di Biagio et al., 2017; Gaiero et al., 2007; Gaiero et al., 2003; Qu, 2016), although there is also some data from the Atacama Desert in northern Chile (Di Biagio et al., 2017; Engelbrecht et al., 2016; Rojas et al., 1990), and from a few remote locations in Argentina, Bolivia, and Brazil (Rojas et al., 1990). In Australia, most observations originate from the arid interior of the continent, with main dust source areas located within the Lake Eyre Basin (Box et al., Jan 27-29 2010; Di Biagio et al., 2017; Engelbrecht et al., 2016; Karlson et al., 2014; Moreno et al., 2008; Radhi et al., 2010b, a). These studies focus on ground-based observations of dust aerosols or laboratory-generated aerosols derived from parent soils (Table S2).

To represent Northern African dust, we selected studies on laboratory-generated aerosols or aerosols collected in source areas. These include laboratory measurements by Di Biagio et al. (2017) and Engelbrecht et al. (2016), as well as ground based and airborne observations from key aircraft campaigns: the African Monsoon Multidisciplinary Analysis (AMMA, Rajot et al., 2008; Reeves et al., 2010); the Dust And Biomass-burning Experiment (DABEX, Haywood et al., 2008); the Dust Outflow and Deposition to the Oceans (DODO, McConnell et al., 2008); the FENNEC - Saharan Climate System (Washington et al., 2012); and the Geostationary Earth Radiation Budget Intercomparisons of Longwave and Short−wave radiation (GERBLIS, Haywood et al., 2011).

3 Results

3.1 Elemental Composition

Figure 2 shows the percentage of the major crustal elements found in different types of SAf dust grouped by source region. Note that the Kalahari samples collected across Botswana have been grouped into the Kalahari BOT dataset. The most abundant element is Si, which varies significantly, ranging from around 35 wt% in the Kalahari BOT samples to 18 wt% at Etosha Pan. Al content is highest in the riverbed dust, reaching up to 13 wt%. The riverbed dust also has the highest Fe content (up to 9 wt%) along with dust from savannah soils at Skukuza, whereas the Etosha Pan dust contains less than 1 wt% of Al and Fe. On the other hand, mineral dust from the Etosha Pan has the highest concentrations of Ca and Mg, each around 17 wt%, and about 4 wt% Na. In the riverbed, Namib GP, and Hope Mine samples, the levels of Ca, Mg, and Na are lower but still significant, ranging from 4.5 wt% to 17 wt% overall. Samples from the Free State, Kalahari BOT, and Skukuza show the lowest total contents, ranging from 0.6 wt% to 3.7 wt%.

https://doi.org/10.5194/egusphere-2026-1532
Preprint. Discussion started: 30 March 2026

The riverbed dust contains the highest K concentrations, ranging from 2.4 wt% to 3.6 wt%, while in the Kalahari BOT samples, K varies from 0 to 3 wt%, with the highest level observed in the sample from south of the Okavango Delta.

Hope Mine dust is notably rich in Cu, approximately 8 wt% (not shown), and also contains a high level of P at 0.3 wt%. P varies from 0.02 wt% to 0.2 wt% in the other dust samples, but was not detected in the Etosha Pan dust. The riverbed dust is slightly richer in Ti (up to 0.9 wt%) compared to the other dust samples, while Mn shows no significant variability across the samples. Neither of these elements was detected in the Etosha Pan dust.

3.2 Mineralogy

The main minerals in SAf dust aerosols are quartz and clays, while carbonates and feldspars are only present in some samples. The limited aerosol mass results in low diffractogram intensity relative to the baseline, which complicates the identification of minor mineral species. For instance, Fe oxide minerals, gypsum (CaSO4·2H2O), and halite (NaCl) have been identified in a few samples, mostly in small quantities. The fact that these minor phases were not detected by XRD can have two reasons: (1) the phases contain crystalline defects or are even amorphous (like certain iron oxides), (2) the very low number of crystals present reduces the likelihood of planes oriented in a way that allows their diffraction. The detection limit for X-ray diffraction is generally estimated to be a few per cent by mass. Therefore, the presence or absence of these minerals cannot be definitively confirmed, and further characterisation using alternative techniques is recommended. The same consideration applies to apatite ($Ca_5(PO_4)_3(F, Cl, OH)$), which could be present given the relatively good correlation between Ca and P (Figs. S2-S4), although it was not detected by XRD.

Figure 3 reports key mineral components of SAf dust aerosols. Dust aerosol samples generated from sandy soils collected across the Kalahari BOT and in the Free State have the highest quartz content, ranging from 26 wt% to 37 wt%. The remaining samples contain less than 15 wt% quartz, while quartz was not detected in mineral dust from the Etosha Pan, where carbonates (as the total contribution of calcite, $CaCO_3$, and dolomite, $CaMg(CO_3)_2$) dominate at 78 wt%. A carbonate content of up to 20 wt% was also observed in mineral dust from arid coastal regions, including the Namib GP and ephemeral riverbeds. The feldspar content, calculated as the sum of albite ($Na(AlSi_3O_8)$) and microcline ($K(AlSi_3O_8)$), is highest in dust from savannah soils (over 30 wt%), followed by riverbed dust (10-30 wt%), the Kalahari BOT sample from the south of the Okavango Delta (20 wt%), Namib GP dust (over 10 wt%), Free State dust (2 wt%), and not detected in other samples.

Dust aerosols are mostly composed of clay minerals, ranging from 20 wt% (Etosha Pan) to 50-90 wt% (other SAf dust). The clay minerals observed include illite ($K_{0.6-0.85}(Al,Mg)_2(Si,Al)_4O_{10}(OH)_2$), kaolinite ($Al_2(Si_2O_5)(OH)_4$), Mg-rich clays (i.e. sepiolite, $Mg_4(Si_6O_{15})(OH)_2·6H_2O$, and palygorskite, $(Mg,Al)_2Si_4O_{10}(OH)·4H_2O$), chlorite ($(Mg, Fe)_3(Si,Al)_4O_{10}(OH)_2·(Mg,Fe)_3(OH)_6(Fe,Mg)_2Al_4O_2(SiO_4)_2(OH)_4$), chrysocolla ($Cu_4,H_4Si_4O_{10}(OH)_8$), and montmorillonite ($(Al,Mg)_8(Si_4O_{10})_4(OH)_8·12H_2O$), all of which reveal specific regional features.

The abundance of kaolinite indicates highly weathered soils and tends to follow rainfall patterns (Fig. 4). Arid areas close to the Namibian coast and the Kalahari BOT sample from the southwestern Kalahari have the lowest kaolinite content, while illite-like clays (represented by the sum of illite and muscovite, $KAl_2(AlSi_3O_{10})(OH)_2$) dominate due to low chemical

https://doi.org/10.5194/egusphere-2026-1532
Preprint. Discussion started: 30 March 2026

weathering. Kaolinite content increases from south to north in the Kalahari BOT samples, reaching over 40 wt% of the total clay in the sample collected north of the Okavango Delta, an area that receives the highest levels of precipitation. Agricultural soils in the Free State, inland South Africa, and savannah soils in eastern South Africa receive more precipitation than coastal Namibia, with kaolinite accounting for 20-50 wt% of the total clay fraction in dust. Lastly, kaolinite accounts for over 30 wt% of the clay fraction in the mineral dust from the copper mine, which also contains a significant amount of chrysocolla, a Cu-rich clay, and around 8% Fe oxide minerals.

Mg-rich clays such as sepiolite and palygorskite can form in arid and semi-arid environments with alkaline soils, high Mg activity, and evaporation, like in lacustrine and peri-marine zones (Singer, 2002). They can also form through meteoric or hydrothermal alteration of basic rocks, or as a result of pedogenic processes in soils, such as the formation of calcareous crusts (Singer, 2002). The presence of sepiolite and palygorskite is documented in sediments of Etosha Pan (Buch and Rose, 1996) and in sediments of the Central Namib Gravel Plain, including riverbeds (Heine and Völkel, 2010). Here, we observed that dust from Etosha Pan is characterised by a high Mg-rich clay content, accounting for around 50% of its total clay composition. Mg-rich clays are also present in smaller amounts in dust from riverbeds, Namib GP, and savannah soils (Fig. 3). Lastly, samples from the Namib GP and the Kuiseb riverbed contain around 10 wt% chlorite and 1 wt% montmorillonite (not shown).

These results align with potential mineral associations indicated by the correlation between crustal elements (Figs. S2-S4). A strong correlation was observed between Al and Si, as well as between Al and Si with Fe, K, Ti, P, and Mn ($r > 0.7$), suggesting an association with aluminosilicate minerals, such as feldspars, clays, and Fe-Ti oxides. The concentrations of Ca and Mg are strongly correlated ($r \approx 0.8$), while their correlations with Fe, Si, and Al are weaker ($r \leq 0.4$). The weak correlation of Ca and Mg with Al suggests that these elements can be associated with different minerals depending on the source. For instance, they are mainly associated with calcite and palygorskite in Namib GP and riverbed samples, with dolomite and sepiolite in Etosha Pan, and with other aluminosilicate minerals in the remaining dust samples. This indicates that (Ca+Mg)/Al is a good discriminating indicator of SAf dust sources. Additionally, Na shows a strong correlation with Mg ($r = 0.8$) and a moderate correlation with Ca ($r = 0.6$), indicating a common source and/or similar geochemical processes. This may suggest that some Ca and Mg derive from minor evaporitic salts.

The abundance of P is often associated with phosphate minerals such as apatite. Our findings show that P is moderately correlated with Ca ($r \approx 0.5$), thus suggesting the presence of apatite. However, its strong correlations with Si, Al, and Fe suggest that P is probably associated with clay minerals and Fe and Al oxides.

https://doi.org/10.5194/egusphere-2026-1532
Preprint. Discussion started: 30 March 2026

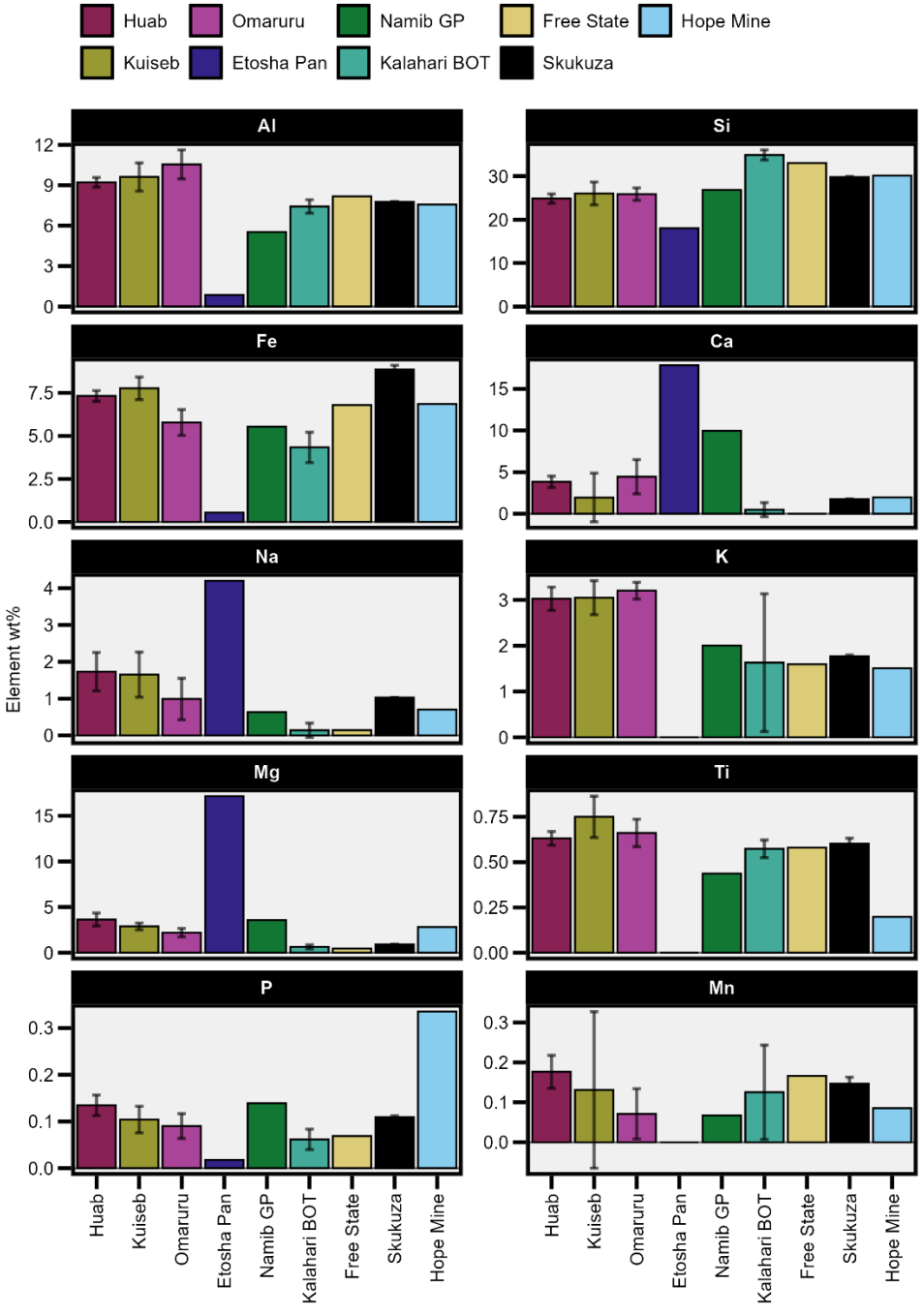

Figure 2. Fractions of crustal elements (wt%) in SAf dust aerosols by source region. Standard deviations are calculated from multiple samples; if not shown, this indicates that only a single sample was available. Samples collected across Botswana from the Kalahari are grouped into the Kalahari BOT dataset. Namib GP refers to the Central Namib Gravel Plain.

https://doi.org/10.5194/egusphere-2026-1532
Preprint. Discussion started: 30 March 2026

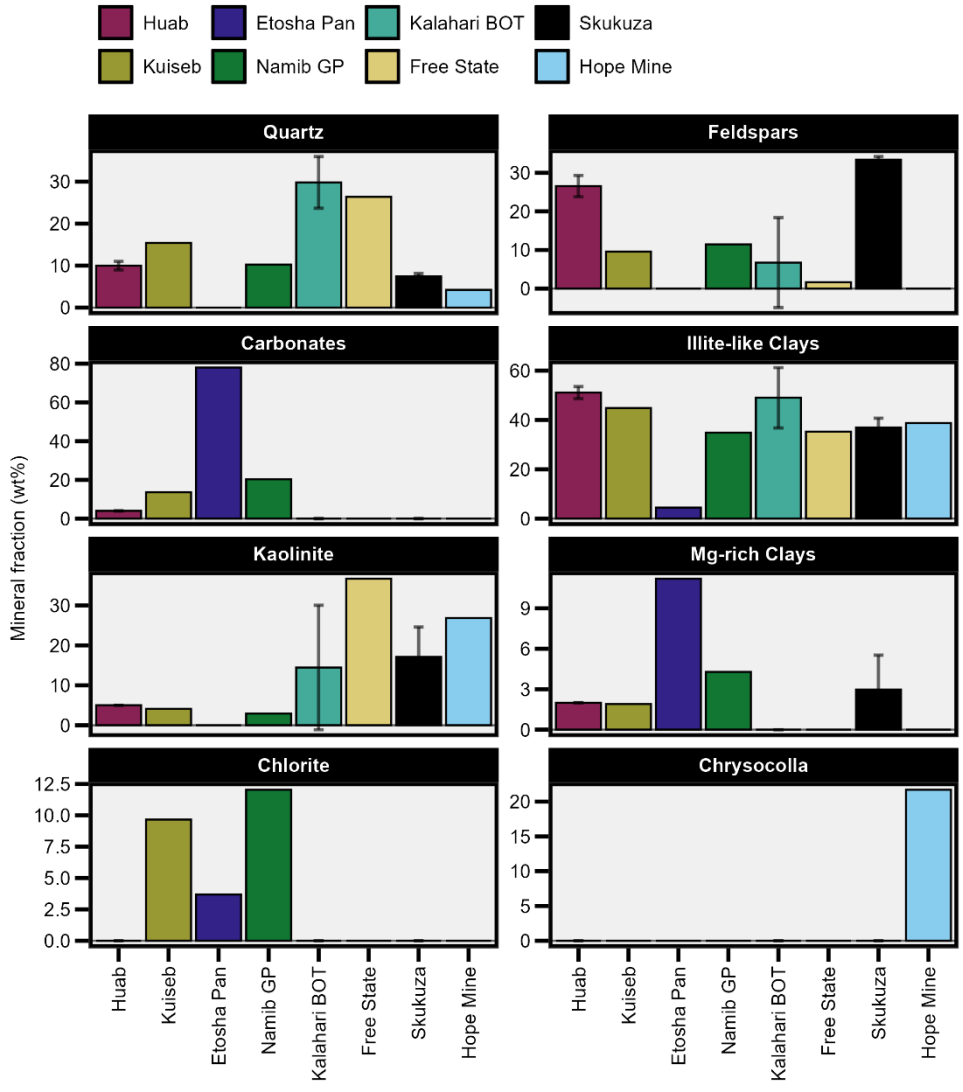

Figure 3. Main mineral components of SAf dust aerosols by source region. Standard deviations are calculated from multiple samples; if not shown, this indicates that only a single sample was available. Samples collected across Botswana from the Kalahari are grouped into the Kalahari BOT dataset. Namib GP refers to the Central Namib Gravel Plain. Illite-like clays are calculated as the sum of illite and muscovite, Mg-rich clays as the sum of sepiolite and palygorskite, carbonates as the sum of calcite and dolomite, and feldspars as the sum of microcline and albite. The mineralogy of the Omaruru riverbed samples could not be determined because insufficient dust mass was collected for XRD analysis during laboratory experiments at CESAM.

https://doi.org/10.5194/egusphere-2026-1532
Preprint. Discussion started: 30 March 2026

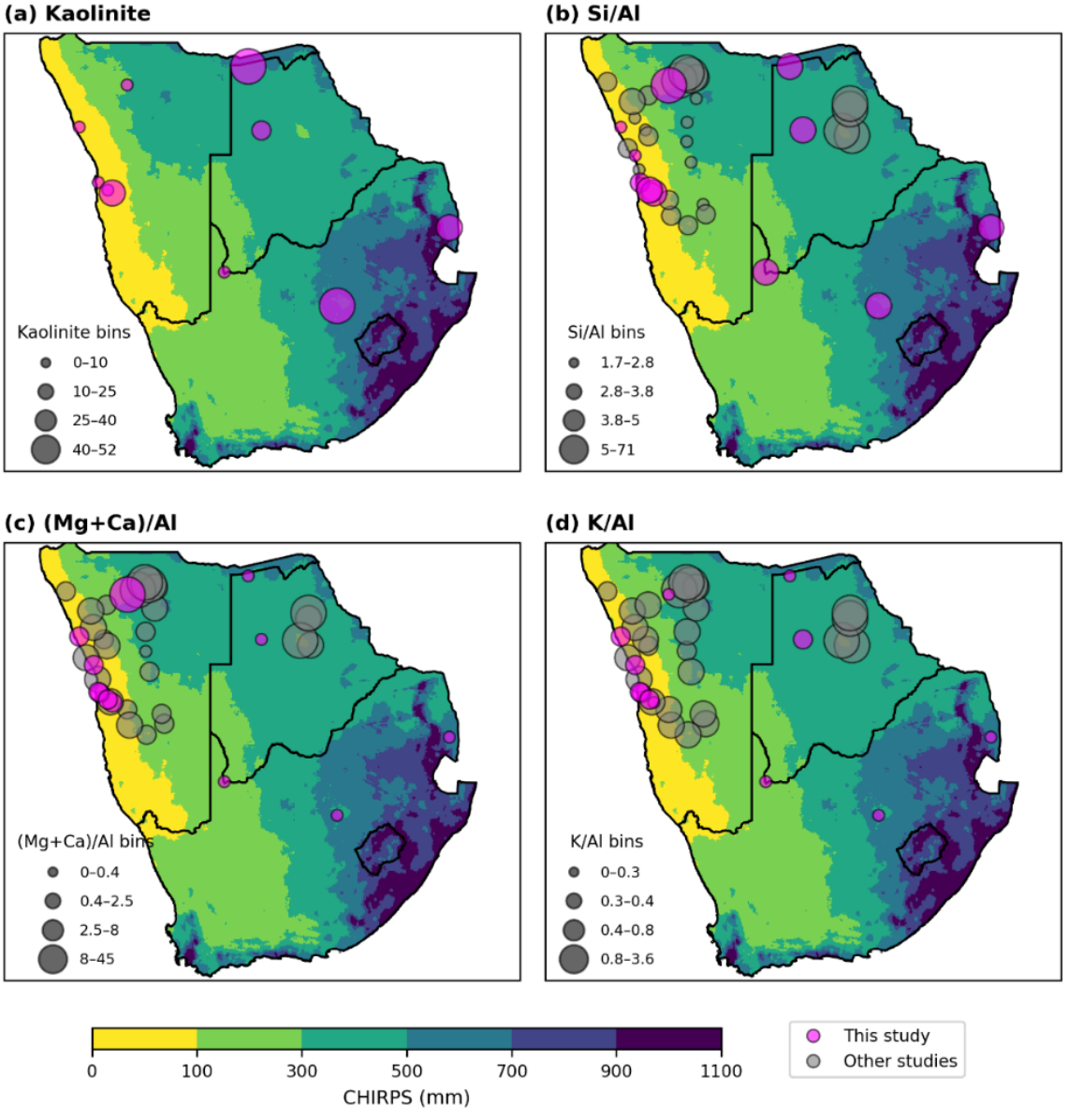

Figure 4. Spatial distribution of Kaolinite, (Ca + Mg)/Al, Si/Al, and K/Al ratios, overlaid on the mean annual precipitation map of Southern Africa. The kaolinite fraction in clays is from this study. For the elemental ratios, Namib GP data include this study, Di Biagio et al. (2017), and Qu (2016). Kalahari NAM data are from Qu (2016). Salt Pans data include this study and Engelbrecht et al. (2016). Data source references for elemental ratios are summarised in Table S2. The rainfall map is generated from CHIRPS v3 (CHIRPS3, 2025) data (see Text S2 for additional details on CHIRPS v3 source data). The bin sizes of chemical parameters were selected to better highlight the geochemical characteristics of various mineral dust sources, which are described and discussed in section 4.1 of the main text. Note that for the Huab, Kuiseb, and Omaruru rivers, only the average ratios are presented.

https://doi.org/10.5194/egusphere-2026-1532
Preprint. Discussion started: 30 March 2026

4 Discussion

Our data reveal distinct chemical and mineralogical characteristics among SAf dust sources. Combining our findings with existing literature, we provide an overview of the compositional variability of mineral dust across Southern Africa. We also compare the elemental enrichment and key minerals in SAf dust with other major dust sources in the Southern Hemisphere, and in Northern Africa, the major global dust source, and assess potential atmospheric implications.

4.1 Compositional variability of SAf dust based on elemental ratios and mineral indicators

The elemental ratios, primarily Si/Al, (Ca+Mg)/Al, and K/Al, are critical tracers of mineral dust that can be used to distinguish source areas across Southern Africa. Significant associations were identified and are reported in Fig. S5 based on comparisons of these chemical ratios with the dust mineralogy. The K/Al ratio shows a direct correlation with K-feldspar (microcline) and an inverse correlation with kaolinite, a mineral produced by the chemical weathering of aluminosilicate minerals, including feldspars. The Si/Al ratio increases with quartz and decreases with increasing primary aluminosilicate mineral contents (feldspar and muscovite). The (Ca + Mg)/Al ratio is directly correlated with carbonate mineral content and Mg-rich clay content, which formed in similar geochemical environments.

Figure 5 illustrates the variability in the chemical composition of mineral dust across Southern Africa, presenting the Si/Al, (Ca+Mg)/Al, K/Al, and Fe/Al ratios from this study and laboratory-generated dust aerosols from the literature (Di Biagio et al., 2017; Engelbrecht et al., 2016; Qu, 2016). The data were grouped into spatial-environmental categories based on their geographic location and geomorphological environment (Table S3). Additionally, we compared the elemental ratios of laboratory-generated mineral dust aerosols with atmospheric observations over coastal Namibia, which is representative of dust mixed aerosols in a marine coastal environment (Desboeufs et al., 2024; Formenti et al., 2025; Klopper et al., 2020), and the South African Highveld, representative of dust mixed aerosols in an inland urban-industrial environment (Baldo et al., 2025). Both areas are influenced by a range of natural and anthropogenic emissions.

Mineral dust found in the salt pans in Namibia and Botswana exhibits highly variable compositions, but can be distinguished by its elevated (Ca + Mg)/Al ratios (from 3 to 43) and Si/Al ratios (from 5 to 70), reflecting the predominance of carbonates and Mg-rich clays. The K/Al ratios (from 0.9 to 3.6) are also the highest reported in the literature. However, K was not detected in the Etosha Pan sample analysed in this study, indicating variability in the composition of dynamic pan surfaces.

In the case of the Namib GP, the Si/Al ratio is restricted to between 2.8 and 4.8, while the (Ca + Mg)/Al ratio varies between 0.5 and 7.7. In the areas of the Namib GP that are closer to the west coast, the mineral dust (Ca + Mg)/Al ratio is usually greater than 2.5. However, in the eastern part of the Namib GP and in the Kalahari NAM, this ratio falls below 2.5, while the Si/Al ratio decreases to 1.7-3.2. Aerosol samples collected near areas characterised by carbonate-rich rocks and sediments, such as the Etosha Pan and the Otavi Mountain Land in northern Namibia, show higher ratios. The (Ca + Mg)/Al and Si/Al ratios measured in mineral dust from ephemeral riverbeds are closer to those observed in the eastern Namib GP and Kalahari NAM. However, these riverbeds fall within the lower end of the K/Al ratio range observed in these areas: 0.3-0.7.

https://doi.org/10.5194/egusphere-2026-1532
Preprint. Discussion started: 30 March 2026

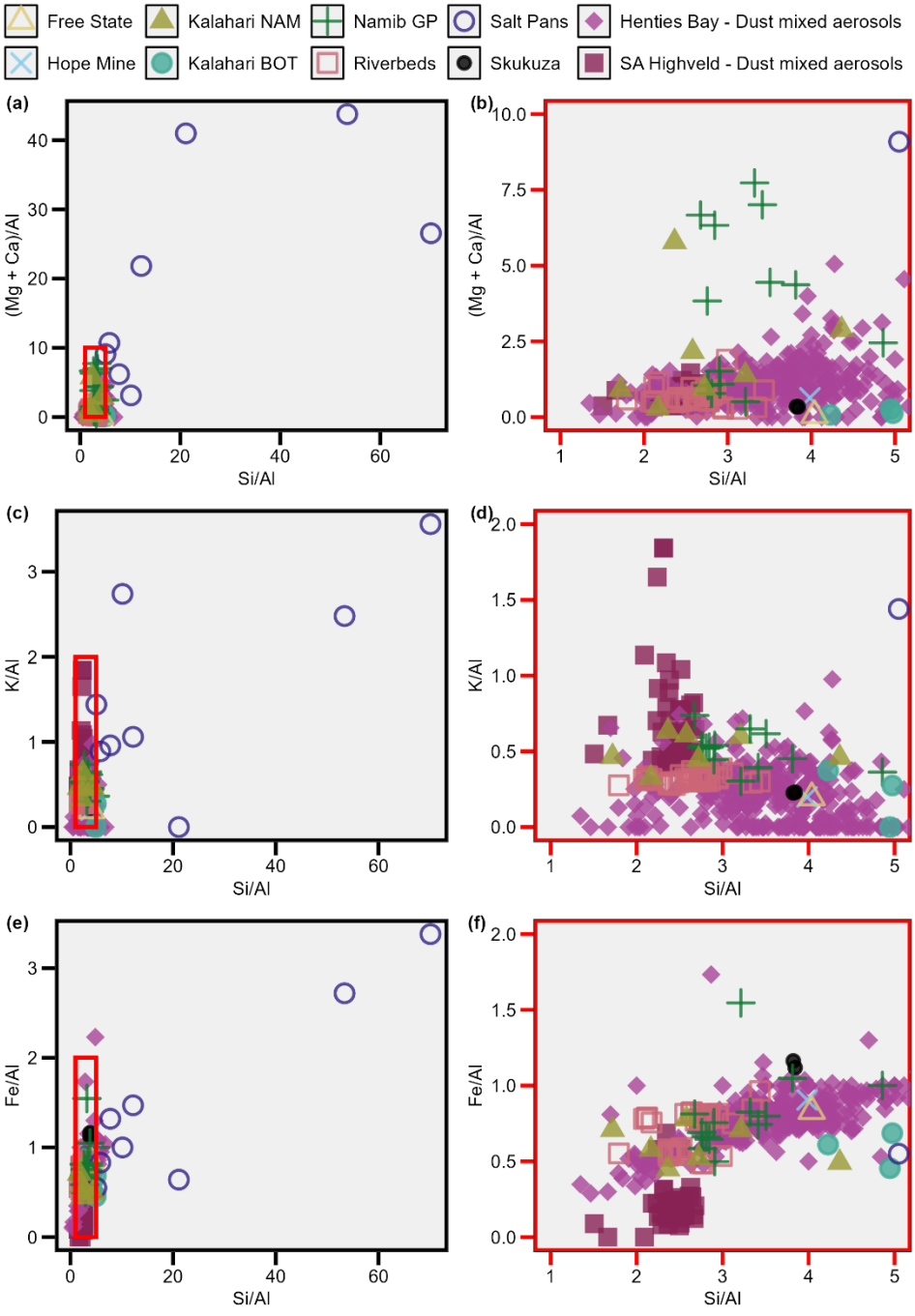

Figure 5. Mineral dust tracer variability across Southern Africa. The red rectangle indicates the zoomed area in the right-hand panels. For the reader's sake, the error bars are not shown. Namib GP data include this study, Di Biagio et al. (2017), and Qu (2016). Kalahari NAM data are from Qu (2016). Salt Pans data include this study and Engelbrecht et al. (2016). Ground-based observations of dust mixed aerosols over the Namibian coast (Desboeufs et al., 2024; Formenti et al., 2025; Klopper et al., 2020) and the South African Highveld (Baldo et al., 2025) are included for comparison. Data source references are summarised in Table S3.

https://doi.org/10.5194/egusphere-2026-1532
Preprint. Discussion started: 30 March 2026

Mineral dust from the Kalahari BOT, agricultural soils in the Free State, and savannah soils at Skukuza differ from other SAf dust due to their low (Ca + Mg)/Al ratios (0.1-0.4). This is consistent with the absence of carbonate minerals, as indicated by XRD analysis. These samples also exhibit relatively higher Si/Al ratios of 3.8-4.9, reflecting an increase in quartz and a decrease in primary aluminosilicate minerals compared to the Namibian dust (Fig. 3). Overall, mineral dust originating from inland eastern sources (the Botswana section of the Kalahari Desert, the Free State, and Skukuza) has lower K/Al values than dust from Namibia (below 0.4). This is consistent with the observed increase in kaolinite content, which is attributed to increased chemical weathering in the parent sediments. Mineral dust from the copper mine has similar (Ca + Mg)/Al, Si/Al, and K/Al ratios to those of the inland eastern sources, but can be readily distinguished by its high Cu content (8 wt%).

These three crustal element ratios alone are insufficient to distinguish inland eastern sources. However, mineral dust from Skukuza and the Free State can be distinguished by their high Fe content (Fig. 2), as reflected in elevated Fe/Al ratios of 0.8-1.2 (Figs. 5e-f). Additionally, differences in kaolinite content help to distinguish between regions from north to south within the Kalahari BOT area (Figs. 3 and 4).

Figure 4 shows the spatial distribution of kaolinite, (Ca + Mg)/Al, Si/Al, and K/Al ratios overlaid on a mean annual precipitation map of Southern Africa. This map is based on the annual average precipitation data for 2015-2024 from the Climate Hazards Center Infrared Precipitation with Stations dataset version 3 (CHIRPS3, 2025). Additional details on the rainfall source data are provided in Text S2. Overall, mineral dust sources in Namibia exposed to more arid environments tend to have lower kaolinite and Si/Al ratios, but higher (Mg + Ca)/Al and K/Al ratios compared to sources further inland and to the east, which receive more precipitation. The Etosha and Makgadikgadi Pans stand out for their very distinctive compositions. Variations between source areas are also affected by differences in geological and geomorphological settings.

Ground-based observations of SAf aerosols are influenced by sources other than mineral dust, such as marine emissions along the Namibian coast (Desboeufs et al., 2024; Formenti et al., 2025; Klopper et al., 2020). To remove the marine aerosol contribution from data reported at the Henties Bay site (Desboeufs et al., 2024; Formenti et al., 2025; Klopper et al., 2020), the concentrations of K, Ca, and Mg were apportioned into sea salt (ss) and non-sea salt (nss) fractions using the nominal mass ratio to Na^+ in seawater, as in Klopper et al. (2020). Thus, the ratios shown in Fig. 5 for Henties Bay are the nss-element fractions relative to Al. No significant influence of marine emissions was observed in aerosols collected from the Southern African Highveld (Baldo et al., 2025). The chemical composition of aerosols from both Henties Bay and the South African Highveld remains affected by anthropogenic emissions (Baldo et al., 2025; Desboeufs et al., 2024; Formenti et al., 2025; Klopper et al., 2020).

The (Ca + Mg)/Al and Si/Al ratios from ground-based observations are consistent with those of mineral dust aerosols analysed in this study and previous research (Table S3). Atmospheric aerosols over the Namibian coast consist of 20% mineral dust, with (Ca + Mg)/Al ratios ranging from 0 to 5 and Si/Al ratios between 0.5 and 6.8 (Desboeufs et al., 2024; Formenti et al., 2025; Klopper et al., 2020). This indicates that a variety of mineral dust sources, including the eastern Namib GP, riverbeds, and more inland areas, influence the Namibian coastal environment. In contrast, mineral dust accounts for around 60% of aerosol mass over the South African Highveld, with (Ca + Mg)/Al and Si/Al ratios of 0.3-1.5 and 1.5-2.7,

https://doi.org/10.5194/egusphere-2026-1532
Preprint. Discussion started: 30 March 2026

respectively (Baldo et al., 2025), values that are closer to those of mineral dust from the eastern Namib GP and the Kalahari NAM areas.

Other crustal element ratios reported for atmospheric aerosols exhibit greater variability than those of mineral dust sources, likely due to anthropogenic influences. The K/Al ratio, in particular, is affected by biomass burning emissions (Baldo et al., 2025; Desboeufs et al., 2024; Formenti et al., 2025; Klopper et al., 2020), varying up to 1 in atmospheric aerosols over the Namibian coast and up to 1.8 in aerosols over the Highveld. The Fe/Al ratio in atmospheric aerosols over the Namibian coast is consistent with that observed in dust source areas. However, additional sources appear to influence the Fe/Al ratios over the South African Highveld, where the ratios are lower (Figs. 5e-f).

4.2 Element and mineral enrichment in SAF dust compared with global dust sources

Enrichment factors (EFs) were used to analyse differences in elemental enrichment across key mineral dust source regions in the Southern Hemisphere, including Southern Africa, Australia, and Southern America, compared with Northern Africa, the primary global dust source. The reference source data used to compile the integrated dataset of the chemical composition and mineralogy of mineral dust are presented in Table S2.

The availability of data varies unevenly across global source regions. Northern African (NAf) dust accounts for the highest proportion (64%), followed by Southern American (SAm) dust (20%), SAf dust (9%), and Australian (Aus) dust (7%). This reflects the limited availability of mineral dust observations in the Southern Hemisphere. The availability of measured elements in Aus dust is particularly limited. Although Fe, Ti, and Mn were consistently reported in 85% of the compiled measurements, other crustal elements were available for only 16-37%. For SAm, SAf, and NAf dust, crustal element coverage was extensive, ranging from 85% to 100%, except for Mn, which was not quantified in most of the selected studies on NAf dust.

Figure 6 shows the EF values by global dust source region, while Table S4 summarises the relevant statistics. The most abundant element in the Earth's crust, Si, has EF interquartile ranges (IQRs) close to the crustal ratio across all regions, except for NAf dust, which is slightly depleted (Table S4). All dust sources are depleted in Na, ranging from slightly depleted in SAm dust (EF median 0.8) to strongly depleted in NAf dust (EF median 0.02).

SAf dust is enriched in Ca, Mg and K, which are key tracers of carbonate (and Mg-rich clays) and K-feldspar minerals. EF median values in Aus and NAf dust vary from slight depletion to near-crustal levels. In contrast, SAf and SAm dust show slight to moderate enrichment. SAf dust exhibits the broadest range and the highest maximum values of 96, 110, and 12, respectively.

SAf dust is from slightly to moderately enriched in the essential micronutrients Fe, P, and Mn. Median EF values range from 1.6 to 2, with IQRs spanning from 0.95 to 3.3. However, SAm dust shows the highest enrichment in P (median EF: 5.8; IQR: 4.9-7), whereas Aus dust is slightly enriched in Fe (median EF: 1.8; IQR: 1.4-2.2) and Mn (median EF: 1.7; IQR: 1.2-3.2), and NAf dust is only slightly enriched in Mn (median EF: 1.7; IQR: 1.6-2.5).

https://doi.org/10.5194/egusphere-2026-1532
Preprint. Discussion started: 30 March 2026

SAf dust could be important for atmospheric heterogeneous reactions. In addition to being rich in Ca, SAf dust exhibits a wide range of EF values for Ti, with slight to moderate enrichment (median EF: 1.5; IQR: 1.4-2.9). However, SAm dust is the most enriched in Ti (median EF: 4.1; IQR: 3.4-4.9). NAf dust also shows moderate enrichment (median EF: 1.9; IQR: 1.6-2.2).

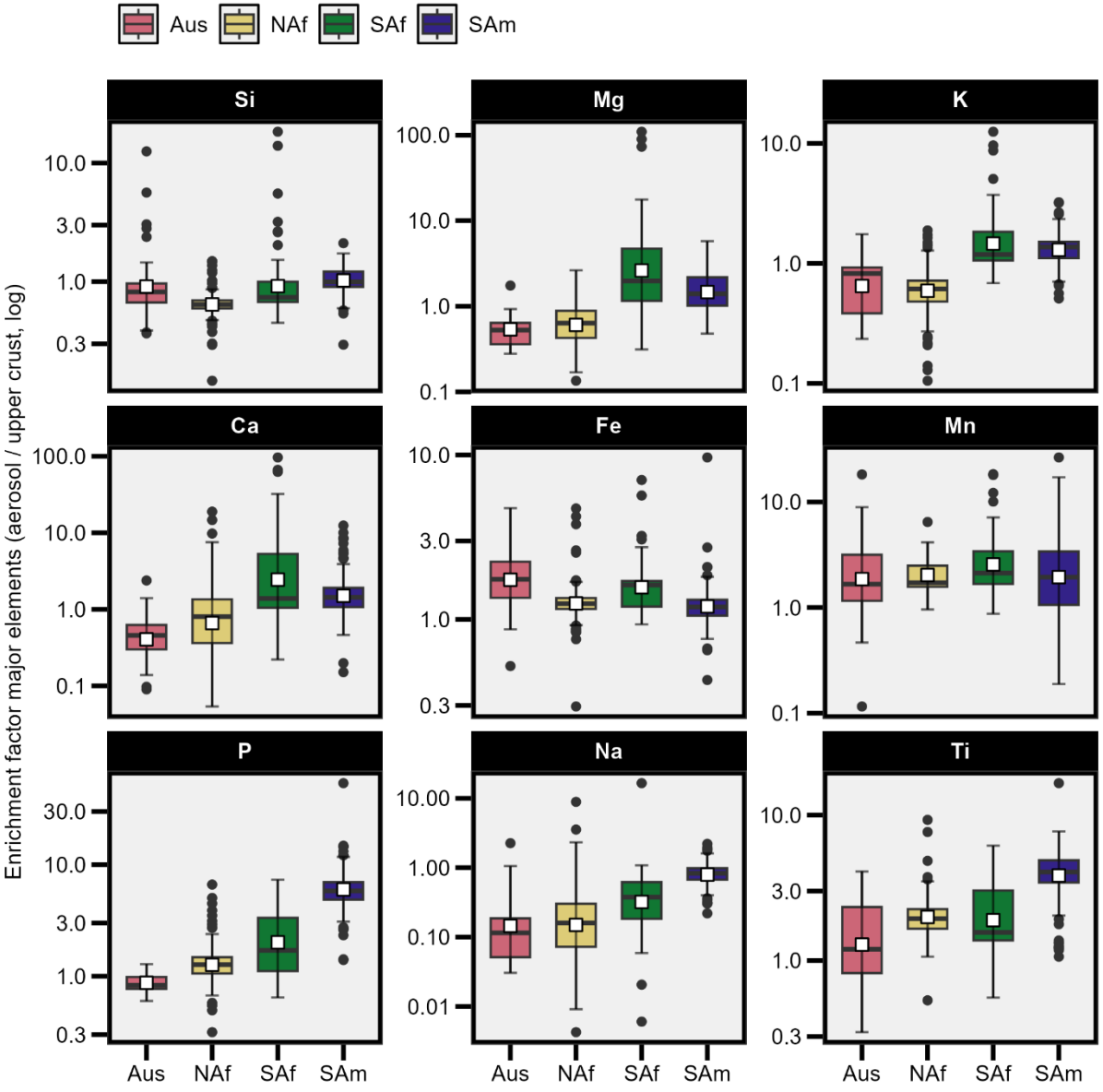

Figure 6. Elemental enrichment factors in mineral dust across Southern Africa (SAf), Australia (Aus), Southern America (SAm), and Northern Africa (NAf). Summary statistics are provided in Table S4. Data source references are provided in Table S2. The white squares show the mean, while the solid lines indicate the median. The lower and upper hinges correspond to the 25th and 75th percentiles, respectively. Whiskers above and below the boxes indicate the 1.5× interquartile range, and values outside this range are plotted individually.

https://doi.org/10.5194/egusphere-2026-1532
Preprint. Discussion started: 30 March 2026

Figure 7 shows the variability of key mineral components in dust particles, including quartz, clays, carbonates, and feldspars, in global dust sources. The integrated mineralogical dataset is still dominated by NAf dust observations; SAf dust accounts for about 22% of the total, and only one observation of Aus dust and two of SAm dust are included. Due to the limited data on Aus and SAm dust, a comprehensive comparison is not possible. Table S5 provides the summary statistics.

Aus and SAm dust sources tend to have higher quartz content than SAf and NAf dust, but the very limited data available do not allow for comparisons that are more meaningful. Notably, there are distinct differences between SAf and NAf dust. SAf dust shows significant enrichment in feldspars, with a median of around 16% and a broad IQR of 2-26%, whereas Naf dust has a median feldspar content of 0.6% and an IQR of 0.4–1%. Conversely, NAf dust exhibits the highest clay content, with a median of 87% and an IQR of 84-91%, compared to SAf dust, which has a median of 60% and an IQR of 67-70%. SAf dust is also more enriched in carbonates (median: 4; IQR: 0-4%) than NAf dust (median: 1; IQR: 0.3-1.9). These findings are consistent with the enrichment of K, Ca, and Mg in SAf dust relative to their depletion in NAf dust (Fig. 6).

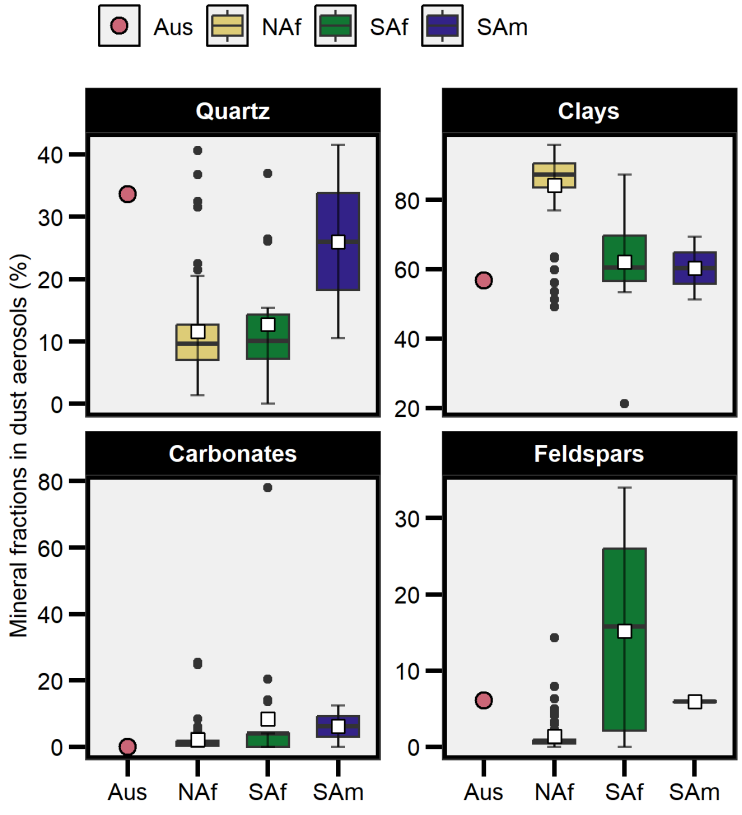

Figure 7. Variability of key mineral components in mineral dust across Southern Africa (SAf), Australia (Aus), Southern America (SAm), and Northern Africa (NAf). Summary statistics are provided in Table S5. Data source references are provided in Table S2 The white squares show the mean, while the solid lines indicate the median. The lower and upper hinges correspond to the 25th and 75th percentiles, respectively. Whiskers above and below the boxes indicate the 1.5× interquartile range, and values outside this range are plotted individually. Only one data point was available for the Australian dust (Aus), which is plotted as an individual point.

https://doi.org/10.5194/egusphere-2026-1532
Preprint. Discussion started: 30 March 2026

5 Conclusions

This study presents new data on the chemical and mineralogical composition of mineral dust aerosols from established dust source regions in Southern Africa and reviews the existing literature on the subject.

Results from the present study show that the crustal element ratios (Mg+Cal)/Al, K/Al, and Si/Al, which serve as key tracers of mineral dust, can distinguish between dust aerosols from more arid western coastal source areas and those from more humid inland eastern source areas. In addition, the clay mineral content provides further information about the source-area environments and the sediment weathering regimes, which are influenced by current and past temperature and precipitation patterns.

Compared to documented major dust sources in the Southern Hemisphere and Northern Africa, SAf dust is enriched in carbonates, which play a significant role in atmospheric heterogeneous reactions, promoting the uptake of gaseous pollutants and the ageing of particles. This results in high hygroscopicity and CCN activity, which may influence the formation of stratocumulus clouds over the northern Bay of Benguela. Additionally, aged SAf particles can contain dissolved essential micronutrients (Fe, P, and Mn), which can impact biogeochemical cycles in marine ecosystems. The high K-feldspar content in SAf indicates high INP activity, which is relevant to mixed-phase clouds over the Southern Ocean, where INP concentrations are low due to the absence of local Antarctic sources.

This study provides the first assessment of the chemical and mineralogical properties of emerging anthropogenic mineral dust sources in Southern Africa, including mining dust, savannah, and agricultural soils. Based on the (Mg+Ca)/Al, K/Al, and Si/Al ratios, no significant differences were observed compared to those of eastern inland sources (Kalahari BOT). However, distinctive features were identified, including Fe enrichment in agricultural and savannah soil samples, feldspar enrichment in savannah samples, and elevated P and Cu levels in mining dust. Additional compositional differences, such as in organic, heavy metal, and rare-earth element content, may exist but will be the focus of a separate study. The small number of anthropogenic mineral dust samples analysed in this study may not capture the variability among different source types, including various agricultural soils, mining ores, road dust, shrublands, and grasslands across Southern Africa, all of which remain unexplored. Further observations are necessary to better characterise these sources, which are becoming increasingly significant in Southern Africa due to climate change and human activity.

Code, data, or code and data availability

The main text and supporting information present data on the chemical composition and mineralogy of Southern African dust. These data will also be made available in the Easy Data repository (www.easydata.earth). In the meantime, they can be obtained from the corresponding author upon request.

https://doi.org/10.5194/egusphere-2026-1532
Preprint. Discussion started: 30 March 2026

Author contributions

CB designed GAMEL experiments with contributions from PF, SL, SC, and KD. PF, AC, JK, NM, and JFD designed CESAM experiments. AC, JK, RS, NM, HCV, GSO, LB, and SP collected samples. CB conducted GAMEL experiments with contributions from SL, SC and CDB. AC, JK, PF, MC, and EP conducted CESAM experiments. SC and GN performed XRF analyses. SN performed XRD analyses with contribution from CB. CB conducted data validation, processing and interpretation with contributions from PF, SN, and SC. CB, PF, SB, AI, SJ, and LB discussed the results. CB drafted the article with contributions from PF. All co-authors reviewed the final text.

Competing interests

The contact author has declared that none of the authors has any competing interests.

Disclaimer

Publisher's note: Copernicus Publications remains neutral with regard to jurisdictional claims made in the text, published maps, institutional affiliations, or any other geographical representation in this paper. While Copernicus Publications makes every effort to include appropriate place names, the final responsibility lies with the authors. Views expressed in the text are those of the authors and do not necessarily reflect the views of the publisher."

Acknowledgements

Contributions to GAMEL experiments by I. Barkai Oumar are gratefully acknowledged. The authors also acknowledge the PRAMMICS Platform of OSU-EFLUVE UAR 3563 and the X-Ray Platform of ITODYS-LISA for access to the instruments. N. Mattielli and R. Stanus jointly thank the FRS-FNRS for the J.0159.25 funding and the ULB-VUB "seed money" grant.

Financial support

This work was partially supported by the Make Our Planet Great Again programme, funded by the French Ministry for Europe and Foreign Affairs, the GEORAD project IdEx/Emergence call, and the OPENDUST Project, IdEx/Crossing Cutting-Edge Call of Université Paris Cité. This research received funding from the French Centre National de la Recherche Scientifique (CNRS) and the South African National Research Foundation (NRF) through the International Research Project "Groupement de Recherche Internationale Atmospheric Research in Southern Africa and the Indian Ocean" (ARSAIO). This work was partially supported by the "PHC GALILEE" programme (project number: 50397UA), funded by the French

https://doi.org/10.5194/egusphere-2026-1532
Preprint. Discussion started: 30 March 2026

Ministry for Europe and Foreign Affairs, the French Ministry for Higher Education and Research and the Italian Ministero dell'Università e della Ricerca (MUR). Akinori Ito acknowledges the Scientific Committee on Oceanic Research (SCOR) for their support of Working Group 167, Reducing Uncertainty in Soluble Aerosol Trace Element Deposition (RUSTED), via a grant to SCOR from the U.S. National Science Foundation (OCE-2513154) and the MEXT Program for the Advanced Studies of Climate Change Projection (SENTAN), Grant Number JPMXD0722681344. This project has received funding fro the TNA activity of the European Union's Horizon 2020 research and innovation programme through the EUROCHAMP-2020 Infrastructure Activity (grant agreement no. 730997). This work has received support under the program "Investissement d'Avenir" launched by the French Government and implemented by ANR, with the reference « ANR-18-IdEx-0001 » as part of its program « Emergence ».

https://doi.org/10.5194/egusphere-2026-1532
Preprint. Discussion started: 30 March 2026

References

Baldo, C., Formenti, P., Nowak, S., Chevaillier, S., Cazaunau, M., Pangui, E., Di Biagio, C., Doussin, J. F., Ignatyev, K., Dagsson-Waldhauserova, P., Arnalds, O., MacKenzie, A. R., and Shi, Z.: Distinct chemical and mineralogical composition of Icelandic dust compared to northern African and Asian dust, Atmospheric Chemistry and Physics, 20, 13521-13539, doi: 10.5194/acp-20-13521-2020, 2020.

Baldo, C., Formenti, P., Di Biagio, C., Lu, G., Song, C., Cazaunau, M., Pangui, E., Doussin, J. F., Dagsson-Waldhauserova, P., Arnalds, O., Beddows, D., MacKenzie, A. R., and Shi, Z.: Complex refractive index and single scattering albedo of Icelandic dust in the shortwave part of the spectrum, Atmospheric Chemistry and Physics, 23, 7975-8000, doi: 10.5194/acp-23-7975-2023, 2023.

Baldo, C., Language, B., Isolabella, T., Vernocchi, V., Massabò, D., van Zyl, P. G., Annegarn, H. J., Piketh, S., and Formenti, P.: Low-Level Urban Anthropogenic Sources Contribute to Strong Aerosol Light Absorption on the South African Highveld, Journal of Geophysical Research-Atmospheres, 130, e2024JD042846, doi: 10.1029/2024jd042846, 2025.

Belelie, M. D., Burger, R. P., von Holdt, J. R. C., Garland, R. M., Liswaniso, G. M., Thomalla, S. J., and Piketh, S. J.: Namib desert dust affects phytoplankton biomass in the Benguela upwelling region: Insights from first mesocosm study, Continental Shelf Research, 285, 105400, doi: 10.1016/j.csr.2024.105400, 2025.

Bhattachan, A., D'Odorico, P., Baddock, M. C., Zobeck, T. M., Okin, G. S., and Cassar, N.: The Southern Kalahari: a potential new dust source in the Southern Hemisphere?, Environmental Research Letters, 7, 024001, doi: 10.1088/1748-9326/7/2/024001, 2012.

Bhattachan, A., D'Odorico, P., Okin, G. S., and Dintwe, K.: Potential dust emissions from the southern Kalahari's dunelands, Journal of Geophysical Research: Earth Surface, 118, 307-314, doi: 10.1002/jgrf.20043, 2013.

Box, M. A., Radhi, M., and Box, G. P.: The great Sydney dust event: size-resolved chemical composition and comparison, in: IOP Conference Series-Earth and Environmental Science, 17th National Conference of the Australian Meteorological and Oceanographic Society, Canberra, AUSTRALIA, Jan 27-29 2010, doi: 10.1088/1755-1315/11/1/012015, 2010.

Bryant, R. G.: Monitoring hydrological controls on dust emissions: preliminary observations from Etosha Pan, Namibia, The Geographical Journal, 169, 131-141, doi: 10.1111/1475-4959.04977, 2003.

Bryant, R. G., Bigg, G. R., Mahowald, N. M., Eckardt, F. D., and Ross, S. G.: Dust emission response to climate in southern Africa, Journal of Geophysical Research-Atmospheres, 112, doi: 10.1029/2005jd007025, 2007.

Buch, M. W., and Rose, D.: Mineralogy and geochemistry of the sediments of the Etosha Pan region in northern Namibia: A reconstruction of the depositional environment, Journal of African Earth Sciences, 22, 355-378, doi: 10.1016/0899-5362(96)00020-6, 1996.

Bullard, J. E.: Arid geomorphology, Progress in Physical Geography: Earth and Environment, 28, 130-144, doi: 10.1191/0309133304pp405pr, 2004.

Caponi, L., Formenti, P., Massabo, D., Di Biagio, C., Cazaunau, M., Pangui, E., Chevaillier, S., Landrot, G., Andreae, M. O., Kandler, K., Piketh, S., Saeed, T., Seibert, D., Williams, E., Balkanski, Y., Prati, P., and Doussin, J. F.: Spectral- and size-resolved mass absorption efficiency of mineral dust aerosols in the shortwave spectrum: a simulation chamber study, Atmospheric Chemistry and Physics, 17, 7175-7191, doi: 10.5194/acp-17-7175-2017, 2017.

https://doi.org/10.5194/egusphere-2026-1532
Preprint. Discussion started: 30 March 2026

Chen, H., Nanayakkara, C. E., and Grassian, V. H.: Titanium dioxide photocatalysis in atmospheric chemistry, Chemical Reviews, 112, 5919-5948, doi: 10.1021/cr3002092, 2012.

Chen, J., Jakob, F. M. O., Voliotis, A., Wu, H., Syafira, S. A., Oghama, O., Shardt, N., Fauré, N., Kong, X., McFiggans, G., and Kanji, Z. A.: Ice Nucleation Abilities and Chemical Characteristics of Laboratory-Generated and Aged Biomass Burning Aerosols, Environmental Science & Technology, 59, 2575-2586, doi: 10.1021/acs.est.4c04941, 2025.

CHIRPS3: Climate Hazards Center Infrared Precipitation with Stations version 3. CHIRPS3 Data Repository https://doi.org/10.15780/G2JQ0P (2025). Data was accessed on [August 2025], in, 2025.

Clem, K. R., Fogt, R. L., Turner, J., Lintner, B. R., Marshall, G. J., Miller, J. R., and Renwick, J. A.: Record warming at the South Pole during the past three decades, Nature Climate Change, 10, 762-770, doi: 10.1038/s41558-020-0815-z, 2020.

Cole, M. J.: A Mine Closure Risk Rating System for South Africa, Mining, 4, 58-78, doi: 10.3390/mining4010005, 2024.

Dansie, A. P., Wiggs, G. F. S., and Thomas, D. S. G.: Iron and nutrient content of wind-erodible sediment in the ephemeral river valleys of Namibia, Geomorphology, 290, 335-346, doi: 10.1016/j.geomorph.2017.03.016, 2017a.

Dansie, A. P., Wiggs, G. F. S., Thomas, D. S. G., and Washington, R.: Measurements of windblown dust characteristics and ocean fertilization potential: The ephemeral river valleys of Namibia, Aeolian Research, 29, 30-41, doi: 10.1016/j.aeolia.2017.08.002, 2017b.

Dansie, A. P., Thomas, D. S. G., Wiggs, G. F. S., and Munkittrick, K. R.: Spatial variability of ocean fertilizing nutrients in the dust-emitting ephemeral river catchments of Namibia, Earth Surface Processes and Landforms, 43, 563-578, doi: 10.1002/esp.4207, 2018.

Degen, T., Sadki, M., Bron, E., König, U., and Nénert, G.: The highscore suite, Powder Diffraction, 29, S13-S18, doi: 10.1017/S0885715614000840, 2014.

Demasy, C., Boye, M., Lai, B., Burckel, P., Feng, Y., Losno, R., Borensztajn, S., and Besson, P.: Iron dissolution from Patagonian dust in the Southern Ocean: under present and future conditions, Frontiers in Marine Science, 11, 1363088, doi: 10.3389/fmars.2024.1363088, 2024.

Derimian, Y., Karnieli, A., Kaufman, Y. J., Andreae, M. O., Andreae, T. W., Dubovik, O., Maenhaut, W., and Koren, I.: The role of iron and black carbon in aerosol light absorption, Atmospheric Chemistry and Physics, 8, 3623-3637, doi: 10.5194/acp-8-3623-2008, 2008.

Desboeufs, K., Formenti, P., Torres-Sánchez, R., Schepanski, K., Chaboureau, J. P., Andersen, H., Cermak, J., Feuerstein, S., Laurent, B., Klopper, D., Namwoonde, A., Cazaunau, M., Chevaillier, S., Feron, A., Mirande-Bret, C., Triquet, S., and Piketh, S.: Fractional solubility of iron in mineral dust aerosols over coastal Namibia: a link to marine biogenic emissions?, Atmospheric Chemistry and Physics, 24, 1525-1541, doi: 10.5194/acp-24-1525-2024, 2024.

Desmet, P. G., and Cowling, R. M.: The climate of the karoo – a functional approach, in: The Karoo: Ecological Patterns and Processes, edited by: Dean, W. R. J., and Milton, S., Cambridge University Press, Cambridge, 3-16, 1999.

Desmet, P. G.: Namaqualand—A brief overview of the physical and floristic environment, Journal of Arid Environments, 70, 570-587, doi: 10.1016/j.jaridenv.2006.11.019, 2007.

https://doi.org/10.5194/egusphere-2026-1532
Preprint. Discussion started: 30 March 2026

Di Biagio, C., Boucher, H., Caquineau, S., Chevaillier, S., Cuesta, J., and Formenti, P.: Variability of the infrared complex refractive index of African mineral dust: experimental estimation and implications for radiative transfer and satellite remote sensing, Atmospheric Chemistry and Physics, 14, 11093-11116, doi: 10.5194/acp-14-11093-2014, 2014.

Di Biagio, C., Formenti, P., Balkanski, Y., Caponi, L., Cazaunau, M., Pangui, E., Journet, E., Nowak, S., Caquineau, S., Andreae, M. O., Kandler, K., Saeed, T., Piketh, S., Seibert, D., Williams, E., and Doussin, J. F.: Global scale variability of the mineral dust long-wave refractive index: a new dataset of in situ measurements for climate modeling and remote sensing, Atmospheric Chemistry and Physics, 17, 1901-1929, doi: 10.5194/acp-17-1901-2017, 2017.

Di Biagio, C., Formenti, P., Balkanski, Y., Caponi, L., Cazaunau, M., Pangui, E., Journet, E., Nowak, S., Andreae, M. O., Kandler, K., Saeed, T., Piketh, S., Seibert, D., Williams, E., and Doussin, J. F.: Complex refractive indices and single-scattering albedo of global dust aerosols in the shortwave spectrum and relationship to size and iron content, Atmospheric Chemistry and Physics, 19, 15503-15531, doi: 10.5194/acp-19-15503-2019, 2019.

Diester-Haass, L., Heine, K., Rothe, P., and Schrader, H.: Late Quaternary history of continental climate and the Benguela Current off South West Africa, Palaeogeography, Palaeoclimatology, Palaeoecology, 65, 81-91, doi: 10.1016/0031-0182(88)90114-9, 1988.

Eckardt, F. D., Bekiswa, S., Von Holdt, J. R., Jack, C., Kuhn, N. J., Mogane, F., Murray, J. E., Ndara, N., and Palmer, A. R.: South Africa's agricultural dust sources and events from MSG SEVIRI, Aeolian Research, 47, doi: 10.1016/j.aeolia.2020.100637, 2020.

Eitel, B., Blümel, W. D., Hüser, K., and Mauz, B.: Dust and loessic alluvial deposits in Northwestern Namibia (Damaraland, Kaokoveld):: sedimentology and palaeoclimatic evidence based on luminescence data, Quaternary International, 76-77, 57-65, doi: 10.1016/s1040-6182(00)00089-6, 2001.

Eltayeb, M. A. H., Vangrieken, R. E., Maenhaut, W., and Annegarn, H. J.: AEROSOL SOIL FRACTIONATION FOR NAMIB DESERT SAMPLES, Atmospheric Environment Part a-General Topics, 27, 669-678, doi: 10.1016/0960-1686(93)90185-2, 1993.

Engelbrecht, F., Adegoke, J., Bopape, M.-J., Naidoo, M., Garland, R., Thatcher, M., McGregor, J., Katzfey, J., Werner, M., Ichoku, C., and Gatebe, C.: Projections of rapidly rising surface temperatures over Africa under low mitigation, Environmental Research Letters, 10, 085004, doi: 10.1088/1748-9326/10/8/085004, 2015.

Engelbrecht, J. P., Moosmüller, H., Pincock, S., Jayanty, R. K. M., Lersch, T., and Casuccio, G.: Technical note: Mineralogical, chemical, morphological, and optical interrelationships of mineral dust re-suspensions, Atmospheric Chemistry and Physics, 16, 10809-10830, doi: 10.5194/acp-16-10809-2016, 2016.

Formenti, P., Rajot, J. L., Desboeufs, K., Caquineau, S., Chevaillier, S., Nava, S., Gaudichet, A., Journet, E., Triquet, S., Alfaro, S., Chiari, M., Haywood, J., Coe, H., and Highwood, E.: Regional variability of the composition of mineral dust from western Africa: Results from the AMMA SOP0/DABEX and DODO field campaigns, Journal of Geophysical Research-Atmospheres, 113, D00C13, doi: 10.1029/2008jd009903, 2008.

Formenti, P., Nava, S., Prati, P., Chevaillier, S., Klaver, A., Lafon, S., Mazzei, F., Calzolai, G., and Chiari, M.: Self-attenuation artifacts and correction factors of light element measurements by X-ray analysis: Implication for mineral dust composition studies, Journal of Geophysical Research: Atmospheres, 115, D01203, doi: 10.1029/2009JD012701, 2010.

Formenti, P., Caquineau, S., Desboeufs, K., Klaver, A., Chevaillier, S., Journet, E., and Rajot, J. L.: Mapping the physico-chemical properties of mineral dust in western Africa: mineralogical composition, Atmospheric Chemistry and Physics, 14, 10663-10686, doi: 10.5194/acp-14-10663-2014, 2014.

https://doi.org/10.5194/egusphere-2026-1532
Preprint. Discussion started: 30 March 2026

Formenti, P., D'Anna, B., Flamant, C., Mallet, M., Piketh, S. J., Schepanski, K., Waquet, F., Auriol, F., Brogniez, G., Burnet, F., Chaboureau, J.-P., Chauvigné, A., Chazette, P., Denjean, C., Desboeufs, K., Doussin, J.-F., Elguindi, N., Feuerstein, S., Gaetani, M., Giorio, C., Klopper, D., Mallet, M. D., Nabat, P., Monod, A., Solmon, F., Namwoonde, A., Chikwililwa, C., Mushi, R., Welton, E. J., and Holben, B.: The Aerosols, Radiation and Clouds in Southern Africa Field Campaign in Namibia: Overview, Illustrative Observations, and Way Forward, Bulletin of the American Meteorological Society, 100, 1277-1298, doi: 10.1175/BAMS-D-17-0278.1, 2019.

Formenti, P., and Di Biagio, C.: Large synthesis of in situ field measurements of the size distribution of mineral dust aerosols across their life cycles, Earth System Science Data, 16, 4995-5007, doi: 10.5194/essd-16-4995-2024, 2024.

Formenti, P., Giorio, C., Desboeufs, K., Zherebker, A., Gaetani, M., Baldo, C., Landrot, G., Montebello, S., Chevaillier, S., Triquet, S., Siour, G., Di Biagio, C., Battaglia, F., Doussin, J. F., Feron, A., Namwoonde, A., and Piketh, S. J.: Elemental composition, iron mineralogy and solubility of anthropogenic and natural mineral dust aerosols in Namibia: a case study analysis from the AEROCLO-sA campaign, EGUsphere, 2025, 1-28, doi: 10.5194/egusphere-2025-446, 2025.

Gaiero, D. M., Probst, J. L., Depetris, P. J., Bidart, S. M., and Leleyter, L.: Iron and other transition metals in Patagonian riverborne and windborne materials: geochemical control and transport to the southern South Atlantic Ocean, Geochimica Et Cosmochimica Acta, 67, 3603-3623, doi: 10.1016/S0016-7037(03)00211-4, 2003.

Gaiero, D. M., Brunet, F., Probst, J.-L., and Depetris, P. J.: A uniform isotopic and chemical signature of dust exported from Patagonia: Rock sources and occurrence in southern environments, Chemical Geology, 238, 107-120, doi: 10.1016/j.chemgeo.2006.11.003, 2007.

Gambe, T. R., Turok, I., and Visagie, J.: The trajectories of urbanisation in Southern Africa: A comparative analysis, Habitat International, 132, 102747, doi: 10.1016/j.habitatint.2023.102747, 2023.

Garzanti, E., Pastore, G., Stone, A., Vainer, S., Vermeesch, P., and Resentini, A.: Provenance of Kalahari Sand: Paleoweathering and recycling in a linked fluvial-aeolian system, Earth-Science Reviews, 224, doi: 10.1016/j.earscirev.2021.103867, 2022.

Gili, S., Vanderstraeten, A., Chaput, A., King, J., Gaiero, D. M., Delmonte, B., Vallelonga, P., Formenti, P., Di Biagio, C., Cazanau, M., Pangui, E., Doussin, J. F., and Mattielli, N.: South African dust contribution to the high southern latitudes and East Antarctica during interglacial stages, Communications Earth & Environment, 3, 129, doi: 10.1038/s43247-022-00464-z, 2022.

Ginoux, P., Prospero, J. M., Gill, T. E., Hsu, N. C., and Zhao, M.: Global-scale attribution of anthropogenic and natural dust sources and their emission rates based on MODIS deep blue aerosol products, Reviews of Geophysics, 50, RG3005 doi: 10.1029/2012rg000388, 2012.

Gittings, J. A., Dall'Olmo, G., Tang, W., Llort, J., Jebri, F., Livanou, E., Nencioli, F., Darmaraki, S., Theodorou, I., Brewin, R. J. W., Srokosz, M., Cassar, N., and Raitsos, D. E.: An exceptional phytoplankton bloom in the southeast Madagascar Sea driven by African dust deposition, Proceedings of the National Academy of Sciences nexus, 3, pgae386, doi: 10.1093/pnasnexus/pgae386, 2024.

Hamilton, D. S., Perron, M. M. G., Bond, T. C., Bowie, A. R., Buchholz, R. R., Guieu, C., Ito, A., Maenhaut, W., Myriokefalitakis, S., Olgun, N., Rathod, S. D., Schepanski, K., Tagliabue, A., Wagner, R., and Mahowald, N. M.: Earth, Wind, Fire, and Pollution: Aerosol Nutrient Sources and Impacts on Ocean Biogeochemistry, Annual Review of Marine Science, 14, 303-330, doi: 10.1146/annurev-marine-031921-013612, 2022.

https://doi.org/10.5194/egusphere-2026-1532
Preprint. Discussion started: 30 March 2026

Harrison, A. D., Whale, T. F., Carpenter, M. A., Holden, M. A., Neve, L., O'Sullivan, D., Vergara Temprado, J., and Murray, B. J.: Not all feldspars are equal: a survey of ice nucleating properties across the feldspar group of minerals, Atmospheric Chemistry and Physics,, 16, 10927-10940, doi: 10.5194/acp-16-10927-2016, 2016.

Haustein, K., Washington, R., King, J., Wiggs, G., Thomas, D. S. G., Eckardt, F. D., Bryant, R. G., and Menut, L.: Testing the performance of state-of-the-art dust emission schemes using DO4Models field data, Geoscientific Model Development, 8, 341-362, doi: 10.5194/gmd-8-341-2015, 2015.

Haywood, J. M., Pelon, J., Formenti, P., Bharmal, N., Brooks, M., Capes, G., Chazette, P., Chou, C., Christopher, S., Coe, H., Cuesta, J., Derimian, Y., Desboeufs, K., Greed, G., Harrison, M., Heese, B., Highwood, E. J., Johnson, B., Mallet, M., Marticorena, B., Marsham, J., Milton, S., Myhre, G., Osborne, S. R., Parker, D. J., Rajot, J.-L., Schulz, M., Slingo, A., Tanré, D., and Tulet, P.: Overview of the Dust and Biomass-burning Experiment and African Monsoon Multidisciplinary Analysis Special Observing Period-0, Journal of Geophysical Research: Atmospheres, 113, doi: 10.1029/2008JD010077, 2008.

Haywood, J. M., Johnson, B. T., Osborne, S. R., Baran, A. J., Brooks, M., Milton, S. F., Mulcahy, J., Walters, D., Allan, R. P., Klaver, A., Formenti, P., Brindley, H. E., Christopher, S., and Gupta, P.: Motivation, rationale and key results from the GERBILS Saharan dust measurement campaign, Quarterly Journal of the Royal Meteorological Society, 137, 1106-1116, doi: 10.1002/qj.797, 2011.

Heine, K., and Völkel, J.: Soil clay minerals in Namibia and their significance for the terrestrial and marine past global change research, African Study Monographs, 40, 31-50, doi: https://www.namibiadigitalrepository.com/items/show/391., 2010.

Humphries, M. S., McCarthy, T. S., Cooper, G. R. J., Stewart, R. A., and Stewart, R. D.: The role of airborne dust in the growth of tree islands in the Okavango Delta, Botswana, Geomorphology, 206, 307-317, doi: 10.1016/j.geomorph.2013.09.035, 2014.

Ito, A., and Miyakawa, T.: Aerosol Iron from Metal Production as a Secondary Source of Bioaccessible Iron, Environmental Science & Technology, 57, 4091-4100, doi: 10.1021/acs.est.2c06472, 2023.

Jickells, T., Boyd, P., and Hunter, K. A.: Biogeochemical Impacts of Dust on the Global Carbon Cycle, in: Mineral Dust: A Key Player in the Earth System, edited by: Knippertz, P., and Stuut, J.-B. W., Springer Netherlands, Dordrecht, 359-384, 2014.

Jones, A., Breuning-Madsen, H., Brossard, M., Dampha, A., Deckers, J., Dewitte, O., Gallali, T., Hallett, S., Jones, R., Kilasara, M., Le Roux, P., Micheli, E., Montanarella, L., Spaargaren, O., Thiombiano, L., Van Ranst, E., Yemefack, M., and Zougmoré, R.: Soil atlas of Africa, European Commission, Publications Office of the European Union, 2013.

Karlson, L. R., Greene, R. S. B., Scott, K. M., Stelcer, E., and O'Loingsigh, T.: Characteristics of aeolian dust across northwest Australia, Aeolian Research, 12, 41-46, doi: 10.1016/j.aeolia.2013.11.003, 2014.

Karydis, V. A., Tsimpidi, A. P., Bacer, S., Pozzer, A., Nenes, A., and Lelieveld, J.: Global impact of mineral dust on cloud droplet number concentration, Atmospheric Chemistry and Physics, 17, 5601-5621, doi: 10.5194/acp-17-5601-2017, 2017.

Kawai, K., and Matsui, H.: Contributions of Dust Source Regions to Ice Nucleating Particles in Mixed-Phase Clouds Simulated with a Global Climate–Aerosol Model, Journal of Climate, 38, 4925-4939, doi: 10.1175/JCLI-D-24-0696.1, 2025.

https://doi.org/10.5194/egusphere-2026-1532
Preprint. Discussion started: 30 March 2026

Klaver, A., Formenti, P., Caquineau, S., Chevaillier, S., Ausset, P., Calzolai, G., Osborne, S., Johnson, B., Harrison, M., and Dubovik, O.: Physico-chemical and optical properties of Sahelian and Saharan mineral dust: in situ measurements during the GERBILS campaign, Quarterly Journal of the Royal Meteorological Society, 137, 1193-1210, doi: 10.1002/qj.889, 2011.

Klopper, D., Formenti, P., Namwoonde, A., Cazaunau, M., Chevaillier, S., Feron, A., Gaimoz, C., Hease, P., Lahmidi, F., Mirande-Bret, C., Triquet, S., Zeng, Z. R., and Piketh, S. J.: Chemical composition and source apportionment of atmospheric aerosols on the Namibian coast, Atmospheric Chemistry and Physics, 20, 15811-15833, doi: 10.5194/acp-20-15811-2020, 2020.

Kok, J. F., Ridley, D. A., Zhou, Q., Miller, R. L., Zhao, C., Heald, C. L., Ward, D. S., Albani, S., and Haustein, K.: Smaller desert dust cooling effect estimated from analysis of dust size and abundance, Nature Geoscience, 10, 274-278, doi: 10.1038/ngeo2912, 2017.

Kok, J. F., Adebiyi, A. A., Albani, S., Balkanski, Y., Checa-Garcia, R., Chin, M. A., Colarco, P. R., Hamilton, D. S., Huang, Y., Ito, A., Klose, M., Li, L. L., Mahowald, N. M., Miller, R. L., Obiso, V., García-Pando, C. P., Rocha-Lima, A., and Wan, J. S.: Contribution of the world's main dust source regions to the global cycle of desert dust, Atmospheric Chemistry and Physics, 21, 8169-8193, doi: 10.5194/acp-21-8169-2021, 2021.

Krueger, B. J., Grassian, V. H., Cowin, J. P., and Laskin, A.: Heterogeneous chemistry of individual mineral dust particles from different dust source regions: the importance of particle mineralogy, Atmospheric Environment, 38, 6253-6261, doi: 10.1016/j.atmosenv.2004.07.010, 2004.

Lafon, S., Sokolik, I. N., Rajot, J. L., Caquineau, S., and Gaudichet, A.: Characterization of iron oxides in mineral dust aerosols: Implications for light absorption, Journal of Geophysical Research: Atmospheres, 111, D21207, doi: 10.1029/2005jd007016, 2006.

Lafon, S., Alfaro, S. C., Chevaillier, S., and Rajot, J. L.: A new generator for mineral dust aerosol production from soil samples in the laboratory: GAMEL, Aeolian Research, 15, 319-334, doi: 10.1016/j.aeolia.2014.04.004, 2014.

Leung, D. M., Kok, J. F., Li, L. L., Lawrence, D. M., Mahowald, N. M., Tilmes, S., and Kluzek, E.: A global dust emission dataset for estimating dust radiative forcings in climate models, Atmospheric Chemistry and Physics, 25, 2311-2331, doi: 10.5194/acp-25-2311-2025, 2025.

Lide, D. R.: CRC Handbook of Chemistry and Physics 1991–1992, CRC Press, Boca Raton, Florida, 1992.

Liu, J., Wang, X., Wu, D., Wei, H., Li, Y., and Ji, M.: Historical footprints and future projections of global dust burden from bias-corrected CMIP6 models, npj Climate and Atmospheric Science, 7, 1, doi: 10.1038/s41612-023-00550-9, 2024.

Liu, M., Matsui, H., Hamilton, D. S., Lamb, K. D., Rathod, S. D., Schwarz, J. P., and Mahowald, N. M.: The underappreciated role of anthropogenic sources in atmospheric soluble iron flux to the Southern Ocean, npj Climate and Atmospheric Science, 5, 28, doi: 10.1038/s41612-022-00250-w, 2022.

Lu, L., Li, L., Rathod, S., Hess, P., Martínez, C., Fernandez, N., Goodale, C., Thies, J., Wong, M. Y., Alaimo, M. G., Artaxo, P., Barraza, F., Barreto, A., Beddows, D., Chellam, S., Chen, Y., Chuang, P., Cohen, D. D., Dongarrà, G., Gaston, C., Gómez, D., Morera-Gómez, Y., Hakola, H., Hand, J., Harrison, R., Hopke, P., Hueglin, C., Kuang, Y.-W., Kyllönen, K., Lambert, F., Maenhaut, W., Martin, R., Paytan, A., Prospero, J., González, Y., Rodriguez, S., Smichowski, P., Varrica, D., Walsh, B., Weagle, C., Xiao, Y.-H., and Mahowald, N.: Characterizing the Atmospheric Mn Cycle and Its Impact on Terrestrial Biogeochemistry, Global Biogeochemical Cycles, 38, e2023GB007967, doi: 10.1029/2023GB007967, 2024.

https://doi.org/10.5194/egusphere-2026-1532
Preprint. Discussion started: 30 March 2026

Lutterotti, L., Matthies, S., and Wenk, H.: MAUD: a friendly Java program for material analysis using diffraction, IUCr: Newsletter of the CPD, 21, 1999.

Matsui, H., Mahowald, N. M., Moteki, N., Hamilton, D. S., Ohata, S., Yoshida, A., Koike, M., Scanza, R. A., and Flanner, M. G.: Anthropogenic combustion iron as a complex climate forcer, Nature Communications, 9, 1593, doi: 10.1038/s41467-018-03997-0, 2018.

Matthaios, V. N., Pope, D., Koutrakis, P., Olopade, C. O., and North, C. M.: The Struggle Against Air Pollution in African Megacities and the Hidden Problems for the Estimation of the Burden of Disease, Global Challenges, 2025, e00108, doi: 10.1002/gch2.202500108, 2025.

McConnell, C. L., Highwood, E. J., Coe, H., Formenti, P., Anderson, B., Osborne, S., Nava, S., Desboeufs, K., Chen, G., and Harrison, M. A. J.: Seasonal variations of the physical and optical characteristics of Saharan dust: Results from the Dust Outflow and Deposition to the Ocean (DODO) experiment, Journal of Geophysical Research: Atmospheres, 113, D14S05, doi: 10.1029/2007JD009606, 2008.

Mendelsohn, J. M., Jarvis, A., Mendelsohn, M., and Robertson, T.: Atlas of Namibia: its land, water and life, Namibia Nature Foundation, Windhoek, Namibia, 2022.

Mhlongo, S. E.: Physical hazards of abandoned mines: A review of cases from South Africa, The Extractive Industries and Society, 15, 101285, doi: 10.1016/j.exis.2023.101285, 2023.

Moreno, T., Amato, F., Querol, X., Alastuey, A., and Gibbons, W.: Trace element fractionation processes in resuspended mineral aerosols extracted from Australian continental surface materials, Australian Journal of Soil Research, 46, 128-140, doi: 10.1071/sr07121, 2008.

Nash, D. J., and McLaren, S. J.: Kalahari valley calcretes: their nature, origins, and environmental significance, Quaternary International, 111, 3-22, doi: 10.1016/S1040-6182(03)00011-9, 2003.

Nowak, S., Lafon, S., Caquineau, S., Journet, E., and Laurent, B.: Quantitative study of the mineralogical composition of mineral dust aerosols by X-ray diffraction, Talanta, 186, 133-139, doi: 10.1016/j.talanta.2018.03.059, 2018.

Olivier, J.: Spatial distribution of fog in the Namib, Journal of Arid Environments, 29, 129-138, doi: 10.1016/S0140-1963(05)80084-9, 1995.

Piketh, S. J., and Walton, N. M.: Characteristics of Atmospheric Transport of Air Pollution for Africa, in: Air Pollution: Intercontinental Transport of Air Pollution, edited by: Stohl, A., Springer Berlin Heidelberg, Berlin, Heidelberg, 173-195, 2004.

Qu, Z.: Chemical properties of continental aerosol transported over the Southern Ocean: Patagonian and Namibian sources. , PhD Thesis in Geochemistry. Université Pierre et Marie Curie - Paris VI, 2016., doi: https://theses.hal.science/tel-01349197v1, 2016.

Radhi, M., Box, M. A., Box, G. P., Mitchell, R. M., Cohen, D. D., Stelcer, E., and Keywood, M. D.: Size-resolved mass and chemical properties of dust aerosols from Australia's Lake Eyre Basin, Atmospheric Environment, 44, 3519-3528, doi: 10.1016/j.atmosenv.2010.06.016, 2010a.

Radhi, M., Box, M. A., Box, G. P., Mitchell, R. M., Cohen, D. D., Stelcer, E., and Keywood, M. D.: Optical, physical and chemical characteristics of Australian continental aerosols: results from a field experiment, Atmospheric Chemistry and Physics, 10, 5925-5942, doi: 10.5194/acp-10-5925-2010, 2010b.

https://doi.org/10.5194/egusphere-2026-1532
Preprint. Discussion started: 30 March 2026

Rajot, J. L., Formenti, P., Alfaro, S., Desboeufs, K., Chevaillier, S., Chatenet, B., Gaudichet, A., Journet, E., Marticorena, B., Triquet, S., Maman, A., Mouget, N., and Zakou, A.: AMMA dust experiment: An overview of measurements performed during the dry season special observation period (SOP0) at the Banizoumbou (Niger) supersite, Journal of Geophysical Research: Atmospheres, 113, D00C14, doi: 10.1029/2008JD009906, 2008.

Reeves, C. E., Formenti, P., Afif, C., Ancellet, G., Attié, J. L., Bechara, J., Borbon, A., Cairo, F., Coe, H., Crumeyrolle, S., Fierli, F., Flamant, C., Gomes, L., Hamburger, T., Jambert, C., Law, K. S., Mari, C., Jones, R. L., Matsuki, A., Mead, M. I., Methven, J., Mills, G. P., Minikin, A., Murphy, J. G., Nielsen, J. K., Oram, D. E., Parker, D. J., Richter, A., Schlager, H., Schwarzenboeck, A., and Thouret, V.: Chemical and aerosol characterisation of the troposphere over West Africa during the monsoon period as part of AMMA, Atmos. Chem. Phys., 10, 7575-7601, doi: 10.5194/acp-10-7575-2010, 2010.

Rodríguez-Caballero, E., Reyes, A., Kratz, A., Caesar, J., Guirado, E., Schmiedel, U., Escribano, P., Fiedler, S., and Weber, B.: Effects of climate change and land use intensification on regional biological soil crust cover and composition in southern Africa, Geoderma, 406, 115508, doi: 10.1016/j.geoderma.2021.115508, 2022.

Rojas, C. M., Figueroa, L., Janssens, K. H., Vanespen, P. E., Adams, F. C., and Vangrieken, R. E.: THE ELEMENTAL COMPOSITION OF AIRBORNE PARTICULATE MATTER IN THE ATACAMA DESERT, CHILE, Science of the Total Environment, 91, 251-267, doi: 10.1016/0048-9697(90)90302-b, 1990.

Rudnick, R. L., and Gao, S.: 4.1 - Composition of the Continental Crust, in: Treatise on Geochemistry (Second Edition), edited by: Holland, H. D., and Turekian, K. K., Elsevier, Oxford, 1-51, 2014.

Scheuvens, D., Schutz, L., Kandler, K., Ebert, M., and Weinbruch, S.: Bulk composition of northern African dust and its source sediments - A compilation, Earth-Science Reviews, 116, 170-194, doi: 10.1016/j.earscirev.2012.08.005, 2013.

Scheuvens, D., and Kandler, K.: On Composition, Morphology, and Size Distribution of Airborne Mineral Dust, in: Mineral Dust: A Key Player in the Earth System, edited by: Knippertz, P., and Stuut, J.-B. W., Springer Netherlands, Dordrecht, 15-49, 2014.

Scholz, H.: The soils of the central Namib desert with special consideration of the soils in the vicinity of Gobabeb, Madoqua, 1972, 33-51, doi: doi:10.10520/AJA10115498_45, 1972.

Singer, A.: Palygorskite and Sepiolite, in: Soil Mineralogy with Environmental Applications, 555-583, 2002.

Skiles, S. M., Flanner, M., Cook, J. M., Dumont, M., and Painter, T. H.: Radiative forcing by light-absorbing particles in snow, Nature Climate Change, 8, 964-971, doi: 10.1038/s41558-018-0296-5, 2018.

Sokolik, I. N., and Toon, O. B.: Incorporation of mineralogical composition into models of the radiative properties of mineral aerosol from UV to IR wavelengths, Journal of Geophysical Research: Atmospheres, 104, 9423-9444, doi: 10.1029/1998jd200048, 1999.

Storelvmo, T.: Aerosol Effects on Climate via Mixed-Phase and Ice Clouds, Annual Review of Earth and Planetary Sciences, 45, 199-222, doi: 10.1146/annurev-earth-060115-012240, 2017.

Strydom, S., and Savage, M. J.: A spatio-temporal analysis of fires in South Africa, South African Journal of Science, 112, 8, doi: 10.17159/sajs.2016/20150489, 2016.

Stuut, J.-B., W, Crosta, X., van Der Borg, K., and Schneider, R.: Relationship between Antarctic sea ice and southwest African climate during the late Quaternary, Geology, 32, 909, doi: 10.1130/g20709.1, 2004.

https://doi.org/10.5194/egusphere-2026-1532
Preprint. Discussion started: 30 March 2026

Tesfaye, M., Tsidu, G. M., Botai, J., Sivakumar, V., and Rautenbach, C. J. D.: Mineral dust aerosol distributions, its direct and semi-direct effects over South Africa based on regional climate model simulation, Journal of Arid Environments, 114, 22-40, doi: 10.1016/j.jaridenv.2014.11.002, 2015.

Toby, B. H.: R factors in Rietveld analysis: How good is good enough?, Powder Diffraction, 21, 67-70, doi: 10.1154/1.2179804, 2006.

Trisos, C., Adelekan, I., Totin, E., Ayanlade, A., Efitre, J., Gemeda, A., Kalaba, K., Lennard, C., Masao, C., Mgaya, Y., Ngaruiya, G., Olago, D., Simpson, N. P., and Zakieldeen, S.: Africa, in: Climate Change 2022: Impacts, Adaptation and Vulnerability. Contribution of Working Group II to the Sixth Assessment Report of the Intergovernmental Panel on Climate Change [H.-O. Pörtner, D.C. Roberts, M. Tignor, E.S. Poloczanska, K. Mintenbeck, A. Alegría, M. Craig, S. Langsdorf, S. Löschke, V. Möller, A. Okem, B. Rama (eds.)], Cambridge University Press, Cambridge, UK and New York, NY, USA, 2022.

United Nations South Africa: Urgent call to action to address historic El Niño drought in Southern Africa, available at https://southafrica.un.org/en/270894-urgent-call-action-address-historic-el-ni%C3%B1o-drought-southern-africa, (last access: 01 April 2025), 2024.

Vickery, K., and Eckardt, F.: A closer look at mineral aerosol emissions from the Makgadikgadi Pans, Botswana, using automated SEM-EDS (QEMSCAN®), South African Geographical Journal, 103, 7-21, doi: 10.1080/03736245.2020.1824805, 2021.

Vickery, K. J., and Eckardt, F. D.: Dust emission controls on the lower Kuiseb River valley, Central Namib, Aeolian Research, 10, 125-133, doi: 10.1016/j.aeolia.2013.02.006, 2013.

Vickery, K. J., Eckardt, F. D., and Bryant, R. G.: A sub-basin scale dust plume source frequency inventory for southern Africa, 2005-2008, Geophysical Research Letters, 40, 5274-5279, doi: 10.1002/grl.50968, 2013.

von Holdt, J. R., Eckardt, F. D., and Wiggs, G. F. S.: Landsat identifies aeolian dust emission dynamics at the landform scale, Remote Sensing of Environment, 198, 229-243, doi: 10.1016/j.rse.2017.06.010, 2017.

Vos, H. C., Vogel, E., von Holdt, J. R., Fister, W., Eckardt, F. D., Gugger, J. I., Hofstetter, E. C., and Kuhn, N. J.: Arid Shrubland: A growing dust source?, Aeolian Research, 74, 100998, doi: 10.1016/j.aeolia.2025.100998, 2025.

Wang, J., Doussin, J. F., Perrier, S., Perraudin, E., Katrib, Y., Pangui, E., and Picquet-Varrault, B.: Design of a new multi-phase experimental simulation chamber for atmospheric photosmog, aerosol and cloud chemistry research, Atmospheric Measurement Techniques, 4, 2465-2494, doi: 10.5194/amt-4-2465-2011, 2011.

Washington, R., Flamant, C., Parker, D., Marsham, J., McQuaid, J., Brindley, H., Todd, M., Highwood, E., Ryder, C., and Chaboureau, J.: Fennec–the Saharan climate system, CLIVAR Exchanges, 17, 31-33, 2012.

Watson, I., and Lemon, R. R.: Geomorphology of a Coastal Desert: The Namib, South West Africa/Namibia, Journal of Coastal Research, 1, 329–342, 1985.

Wex, H., Eckermann, O., Jurányi, Z., Weller, R., Mangold, A., Van Overmeiren, P., Zeppenfeld, S., van Pinxteren, M., Dall'Osto, M., and Henning, S.: Antarctica's Unique Atmosphere: Really Low INP Concentrations, Geophysical Research Letters, 52, e2024GL112583, doi: 10.1029/2024GL112583, 2025.

Yu, Y., and Ginoux, P.: Enhanced dust emission following large wildfires due to vegetation disturbance, Nature Geoscience, 15, 878-884, doi: 10.1038/s41561-022-01046-6, 2022.

https://doi.org/10.5194/egusphere-2026-1532
Preprint. Discussion started: 30 March 2026

Zolles, T., Burkart, J., Häusler, T., Pummer, B., Hitzenberger, R., and Grothe, H.: Correction to "Identification of Ice Nucleation Active Sites on Feldspar Dust Particles", The Journal of Physical Chemistry A, 123, 6378-6378, doi: 10.1021/acs.jpca.9b05645, 2019.